UNIVERSITY OF CAPE TOWN
IYUNIVESITHI YASEKAPA • UNIVERSITEIT VAN KAAPSTAD

An investigation into the synergistic action of chemotherapy and photodynamic therapy in resistant skin cancers

By:

Fleury Augustin

Nsole Biteghe

Supervisor:

A/Prof Lester M. Davids

Division of Cell Biology
Department of Human Biology
Presented for MSc Proposal (Cell Biology)
Faculty of Health Sciences
University of Cape Town

16th February 2015

PLAGIARISM DECLARATION

1. I know that plagiarism is wrong. Plagiarism is using another's work and to pretend that it is one's own.

2. I have used the American Psychological Association (APA) as the convention for citation and referencing. Each significant contribution to, and quotation in, this essay/report/project/… from the work, or works of other people has been attributed and has cited and referenced.

3. This essay/report/project… is my own work.

4. I have not allowed, and will not allow, anyone to copy my work with the intention of passing it off as his or her own work.

5. I acknowledge that copying someone else's assignment or essay, or part of it, is wrong, and declare that this is my own work

SIGNATURE: _____

DATE: _____

Acknowledgements

Thanks to the Almighty GOD for the blessings and giving me the strength, patience and intelligence to always believe in myself and overcome all my obstacles.

To the incredible A/Prof.Lester Davids, for being not only a supervisor but also a dad, who always help me getting the best out of me. Thank you for all the inspiring and encouraging conversations; it is a blessing to be in your wonderful redox lab.

To the Redox labsters: Ana, Kwezi, Alexis, Toni, Hawa, Meagan, Morea, Mariba, Walley, Desire, Toni and Annesthasia for being such great labmates. I am so grateful to have all of you in my life, thank you for all the supports.

To the T-Box and Kidson lab, for being such helpful and amazing people, you have been my western blot angels.

To Susan cooper for all the microscopy work, you have been such a blessing.

To my family, for the unconditional support, all along the way financially, emotionally and spiritually through prayers, I love you so much!!!!!!!!!!!!!!!!!!!!!!!!!!!!!!!!!!!!

To my Chinese woman from Oyem 'Shalomy', who has been the turning point of my life in this year, thanks for the love, support, lessons about patience, faith and prayers. You are my gift from heaven.

To all my wonderful friends, AKP, Henry (the charmer boy), Odounga family (Desire, Juste and Jean Eudes), Axel Ngwabyt, Mombo Christopher, Emery Mba, Oyabi Christopher, Johan Ondo, Stan Ondo, Davy Ondo, Kenyny, my sisters Djoumessi (vanessa and lutgarde), J-Boy, Rostand and Rubben may GOD keep you all safe!!

To the ''Agence Nationale des bourses du Gabon'' and the ''African Laser Center'' (A.L.C) for the Financial support.

List of Abbreviations

0-6-meG	*0*-6-methylguanine
$^1O_2$	Singlet oxygen
5-ALA	5-Aminolevulinic acid
ABC transporters	ATP-Binding Cassette transporter proteins
AKT	Protein Kinase B
Anti-PD1	Anti-program cell death
BCC	Basal cell carcinoma
BRAF	Proto-oncogene B-Raf
BSA	Bovine Serum Albumin
CANSA	Cancer Association of South Africa
Ce6	Chlorin e6
DMEM	Dulbecco's Modified Eagle's Medium
DMSO	Dimethyl Sulfoxide
DOPA	Dihydroxyphenylalanine
DTIC	Dacarbazine
ECL	Enhanced Chemiluminescence
ER	Endoplasmic reticulum
FDA	United State Food and drug administration
GSH	Reduced Gluthathione
HIF1-α	Hypoxia inducing factor 1-alpha
HYP	Hypericin
HYP-PDT	Hypericin induced Photodynamic therapy
IL-2	Interleukin-2

LDL	Low density lipoproteins
MGMT	*0*-6-methylguanine DNA methyltransferase
MTIC	5-[3-methyltriazen-1yl]-imidazole-4-carboxamide
NBF	Nucleotide binding fold
NK-Cells	Natural killer cells
NMSC	Non melanoma skin cancer
O^-_2	Superoxide anion
$OH^·$	Hydroxyl radical
PBS	Phosphate buffer saline
PDT	Photodynamic therapy
PI3K	Phosphoinositide 3-Kinase
PS	Photosensitizer
RIPA	Radio-immunoprecipitation
ROS	Reactive oxygen species
SDS	Sodium dodecyl sulfate
TBS-T	Tris buffer saline tween
T-Cells	T-lymphocyte cells
TM	Transmenbrane Domain
TYRP1	Tyrosinase related protein 1
TYRP2	Tyrosinase related protein 2
UV	Ultraviolet radiation
VEGF	Vascular endothelial growth factor
XTT	Cell proliferation kit II

Table of Contents

List of Figures and tables

ABSTRACT

Melanoma is a form of skin cancer, arising from epidermal cells of the melanocyte lineage, which undergo a series of transformations and genetic alterations that may give rise to both pigmented and unpigmented melanoma. Melanoma represents 4% of all skin cancers but due to its aggressive nature, it accounts for 80% of death among skin cancer patients. South Africa has a melanoma incidence rate that is second worldwide to only Australia. In melanoma; non-metastatic primary tumours are treated by surgical resection. However, metastatic melanoma is highly resistant to conventional radio and chemotherapy, thus reducing the median life of patient's diagnosis with the metastatic form to about 7-9months. Given the implications of the pigment in failure of chemotherapy, two human metastatic pigmented and unpigmented melanoma cell lines were used to investigate the mechanisms underlying chemo-resistance. During the course of this study, the first aim was to determine the concentration of the chemotherapeutic drug dacarbazine (DTIC) causing fifty percent decrease in melanoma cell viability (LD_{50}), then to investigate the possible synergism of hypericin activated-photodynamic therapy in reducing (HYP-PDT) melanoma cell viability, when combined with chemotherapy. In addition we wanted to assess the morphology and the clonogenic capacity of the melanoma cells, after the different treatments and further investigate the ATP-binding cassette (ABC) transporters (ABCB5/1 & ABCG2) expression profile, before and after chemotherapeutic (DTIC) and combination therapy (DTIC+HYP-PDT) treatments. The results obtained from the cell viability assays, showed that pigmented melanoma was more resistant than unpigmented melanoma after the different treatments at both 24 & 48 hour time points. However, only 48 hour DTIC (1250μM) treatment was shown to kill fifty percent of unpigmented melanoma, while being sub-lethal to their pigmented counterpart. Moreover, at 24 hours, resistance of the pigmented melanoma to chemotherapy was abrogated upon combination therapy treatment (DTIC+ HYP-PDT). This was perfectly correlating with the cell shrinkage (completely disrupted morphology and nuclear aggregate formation in unpigmented cells) and the clonogenic assay, where pigmented melanoma was shown to be more resistant to the chemotherapeutic treatment when compared to their unpigmented counterpart. Significantly, at both 24 and 48 hour time points, HYP-PDT and combination therapies (DTIC+ HYP-PDT) were able to completely suppress the clonogenic capacity of the two metastatic melanoma cells. Lastly, no significant differences in ABCG2/ABCB1/ABCB5 transporter protein expression (at 24 hours) upon DTIC treatment were revealed.

Overall, these results show that melanoma resistance to chemotherapy and combination phototherapies are dependent on the pigmented phenotype of melanoma cells. This work has direct application to further understanding the clinical efficacy of combination treatments in the fight against skin cancer.

Chapter 1: Literature review

1.1. MELANOMA PREVALENCE AND TREATMENTS:

Skin cancer is the most common cancer worldwide[1]. Of the skin cancers, melanoma represents the most aggressive, malignant phenotype resulting from a genetic and/or environmental-induced change to epidermal skin melanocytes. The chief environmental factor remains solar ultraviolet radiation (UV)[2].The melanocytes are located in the basal layer of the skin epidermis, where they produce the pigment melanin, which protects the skin from UV damage (Figure 1). However, it is within the double membrane vesicles called the melanosomes, that melanin are synthesized from the amino acid tyrosine. This, occurs (Dark skin) through the resultant rate-limiting, enzymatic action of the melanocytic enzyme tyrosinase, and the co-ordinated action of tyrosinase related protein 1 (TYRP1) and 2 (TYRP2), resulting in eumelanin production (black-brownish coloured pigment mostly occurring in black) in a processs known as melanogenesis, as opposed to the pheomelanin pigment (yellow-reddish colour) production, which results from nucleophilic oxidation of L-cysteine in presence of dihydroxyphenylalanine (DOPA)[3,4] . Clinically, melanoma can be described as pigmented, characterized by black lesions resulting from melanin accumulation, or unpigmented reflecting a less differentiated cell with less pigment production[5]. In 2000, it was reported that out of 132 000 diagnosed melanoma cases worldwide, melanoma caused 37 000 deaths, highlighting the aggressiveness of the disease[6]. In Europe melanoma caused about 26% of deaths out of the 35000 diagnosed melanoma patients, with shocking statistics recorded in New Zealand and Australia (highest incidence), where melanoma incidence is double the highest incidence rates in Europe, mainly affecting European migrants[6]. South Africa after Australia, has the second highest incidence of melanoma where, 65 and 69 (in the Cape region) new cases respectively per year out of a population of 100, 000 Caucasians are diagnosed[7]. This translates to 1 in 1429 people who will develop malignant melanoma (CANSA Cancer association of South Africa www.melanoma.co.za/D_doccnr _MFS.asp). Interestingly, due to increased public awareness and better dermatological reporting, the trend in South Africa seems to reflect increased cases being reported among the South African black community.

Despite the gold standard for melanoma treatment remaining early detection, surgical excision and adjuvant therapy; the prognosis of metastatic melanoma remains very poor. Once melanomas reach the advanced metastatic stage, they become highly resistant to conventional radiotherapy and chemotherapy[8,9,10]. At this point, melanoma patients are left with a median survival approximating 8 months[11,12,5] and chemotherapy so far has been unsuccessful in improving this survival. Other therapeutic options at this point include therapies such as immunotherapy, biochemotherapy and radiotherapy[13,14].

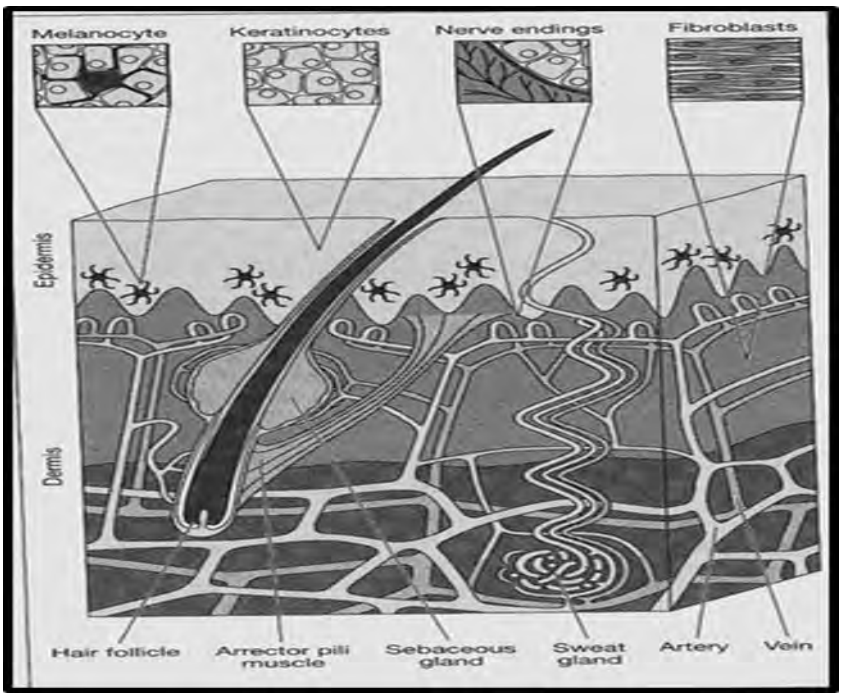

Figure 1: Human skin layers and cell types (adapted from[15])

Currently, the treatment regimens rely on chemotherapy as the best option post-resection with the first U.S food and drug administration approved drug Dacarbazine (DTIC) (1975), used as the standard treatment of metastatic melanoma[16,13,14] To date however, six drugs have been approved by the FDA, for the treatment of metastatic melanoma - dacarbazine (FDA approved in 1975)[14], interleukin-2 (IL-2), vemurafenib, ipilimumab, dabrafenib, and trametinib. Vemurafenib and ipilimumab were FDA approved in 2011, while dabrafenib and trametinib were FDA approved in 2013[17]. Very recently (2014), anti-program cell death-1 (Anti-PD-1), has also been approved for treatment of patients with advanced melanoma[18].

To date single agent chemotherapy using DTIC, have produced the best therapeutic outcome with 15% of patients responding to the therapy, although less than 2% survive 6 years post-treatment[14]. Other proto-oncogene B-Raf (BRAF) inhibiting drugs such as doxorubicin, cisplatin, paclitaxel as well as vemurafenib (FDA approved in 2011)[19] have also been used in the treatment of melanoma and their failures relate to increased cellular toxicity to the surrounding normal cells, development of resistance[9] and their inability to extend survival rate when compared to dacarbazine alone[14,9,20,2122,13]. Given these failures, combination therapies such as biochemotherapy (cytotoxic agents with immunotherapeutic treatment) emerged, in order to attempt to increase the response and survival rates of patients. Thus far, this has shown to be unsuccessful due to the unchanged survival rate of patients and its requirement for safety, of lower dose of IL-2 which compromise the eventuality of complete remission[14]. However, other combination therapies such as DTIC and ipilimumab showed improved patient survival compared to DTIC alone[23].

Although not yet approved by the FDA for melanoma treatment, photodynamic therapy (combination of photosensitizer and visible light) has been effective in the treatment of non-melanoma skin cancer and other cancers[24,25]. It has been tested in vitro for melanoma treatment with promising results, as reported by our laboratory which showed that it potentiated a more pronounced killing of metastatic unpigmented cells, when compared to their pigmented counterparts[26,27]. Moreover, depigmentation of a pigmented metastatic melanoma rendered them more susceptible to cell death induced by the photodynamic treatment (PDT)[27]. This differential response was suggested to be attributed to the pigment melanin, which can affect the PDT efficiency, by either competing for photo-energy or by acting as an antioxidant reducing the reactive oxygen species (ROS) produced by PDT, and in turn, reducing cell death[5,27]. Attempts to circumvent the death resistance, have been tried in melanoma and other cancers by combining PDT and chemotherapy, which have led to promising synergistic actions of the therapies[28,29,30]. In order to understand the failure to the diverse treatments in metastatic melanoma, it would be of great relevance to firstly elucidate the mechanism of actions of the individual therapy (chemotherapy and PDT) and secondly, to understand the resistance mechanisms such as those related to for example the expression of ABC transporters which lower intracellular accumulation of cytotoxic agents.

1.2. PHOTODYNAMIC THERAPY:

1.2.1. Mechanism of action:

It is now well reported that PDT is successful in the treatment of multiple cancers including non-melanoma skin cancers[1,31,32,33]. However, in melanoma, PDT has not yet been approved as a post-resection adjuvant therapy or in combination with other therapies upon metastatic diagnoses. PDT is a minimally invasive two-stage treatment, which involves topical or systemic administration of a photosensitizer (PS), followed by illumination of the tumour or tumorigenic cells with visible light in the presence of molecular oxygen [34,24]. Upon light activation at a specific wavelength, the PS is raised from an unexcited ground state to a very unstable excited triplet state, through absorption of energy in the form of photons. In its triplet state, the PS is unstable and can decay back to its ground state, hence releasing energy to ground state molecular oxygen. This will either result in singlet oxygen ($^1O_2$) formation through a type II photochemical reaction, or upon electron transfer in superoxide anion radical (O^-_2) and hydroxyl radical ($OH^\cdot$) formation via a type I photochemical reaction[24,34] (see Figure 2).

These ROS have a very short half-life (nanoseconds), and exert their cytotoxic effects in the vicinity of their production, as they can diffuse up to only 20nm in cells[34,35]. Upon production, ROS has been shown to be responsible for tumour destruction, activation of anti-tumour immune responses, as well as tumour vasculature damage[32,34]. It follows then that the subcellular localization of the PS is of great relevance, given that ROS production may well cause oxidization of biological molecules such as lipids, proteins and nucleic acids resulting in different modes of cell death[, 34,36,37 ,.38].

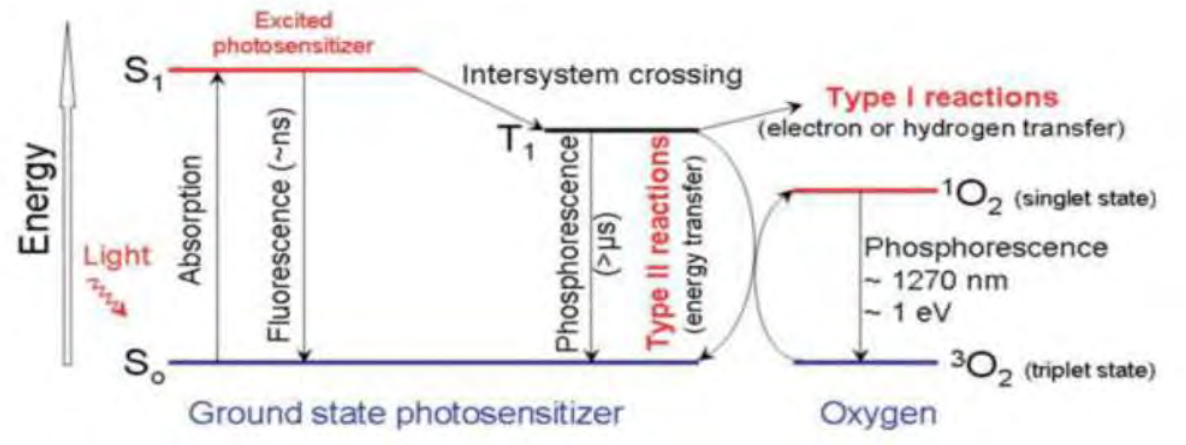

Figure 2: The "trinity" (Photosensitizer, oxygen and light) of photodynamic therapy (PDT).
The photosensitizer moves from the ground singlet state (S0) to an excited singlet state (S1) upon absorption of light. The molecule in S1 may undergo intersystem crossing to an excited triplet state (T1) and then either form radicals via Type I reactions or transfer its energy to molecular oxygen, forming singlet oxygen ($^1O_2$), via Type II reactions. (ns: nanoseconds, µs: microseconds, nm: nanometres, eV: electron volts) modified Jablonski diagram, taken from[24].

1.2.2. Photodynamic therapy and melanoma

PDT is a favorable therapy, which has proven to have negligible toxicity towards normal tissue[39,40], reduced systemic effects, and scarcity of intrinsic or acquired resistance mechanisms. However, in melanoma which is considered to be one of the most unresponsive cancer to known therapies, the use of PDT as a possible adjuvant therapy for the treatment of advanced stages (metastatic) has been investigated, with promising results[5,34]. In 2004, Sheleg et al. reported that complete remission was achieved with no recurrence, on melanoma patients, who were treated with double exposure to Chlorin e6 (Ce6)+ PDT[41]. This was an interesting result, which will necessitate further clinical studies for approval of PDT as melanoma treatment, given the sporadic reports. However, most of the cell death induced mechanisms observed upon melanoma treatment with PDT, involved apoptosis[42,43]. In another study Saczko and colleagues (2005), showed that PDT using photofrin as PS induced apoptosis in 90% of melanoma cells and that the efficacy of the therapy mainly relied on the PS concentration and time of exposure[43]. This was further confirmed by Robertson et al (2010), who showed that activation of 5-aminolevulinic-acid (5-ALA) and

metallophthalocyanine with a light of 680nm and 630nm resulted in growth inhibition of melanoma cells through apoptosis activation[44]. In addition, subcellular localisation of the PS will influence the mode of cell death resulting after PDT, as Choramanska et al (2012) showed that disturbance of the mitochondrial membrane caused by photofrin in Me45 cells induced apoptosis[45].This was recently further emphasized by Kleeman et al. (2014) who found co-localisation of hypericin (PS) within the endoplasmic reticulum (ER), mitochondria, lysosomes and melanosomes[42]. Upon activation with ultraviolet radiation A (UVA), apoptosis was found to be induced via both a caspase-dependent (pigmented & unpigmented melanoma) and independent (moderately pigmented melanoma) pathway. Moreover, earlier work from the same group showed that hypericin-based PDT treatment induced different modes of cell death given the cell types and PS localisation[42,46].

In melanocytes and pigmented melanoma, a necrotic mode of cell death was found as opposed to apoptosis which was observed in keratinocytes and unpigmented melanoma treated with HYP-PDT[46]. From these observations, it was deduced that the necrotic mode of cells death (melanocytes and pigmented melanoma), could be due to increase permeability of the melanosomal membranes, caused by increased ROS production resulting from hypericin activation, which subsequently caused leakage of melanogenesis by-products into the cytoplasm[46]. However, the induction of apoptosis (the moderate /unpigmented melanoma and keratinocytes) was well correlated with a disturbance of the mitochondrial tubular network as well as the loss of structural details of the ER[42,46]. However, no structural modifications were observed in the lysosomes and melanosomes. This observation could well relate to an inherent cellular resistance mechanism to the PDT treatment since both Sharma and Davids (2011) and Chen et al. (2009) demonstrated the protective role of melanin and melanosomes to PDT and chemotherapy[27,47]. This contribution of melanin in reducing PDT efficacy was further reinforced by the demonstration that depigmentation of pigmented melanoma cells (previously resistant to PDT) sensitized them to PDT[27]. In vivo confirmation of this was shown where, using a mouse model, pigmented melanoma was found to be less responsive to PDT than their unpigmented counterpart[48].

Interestingly, the trapping property of anticancer drugs by melanosomes in melanomas (Chen et al., 2009) could be attributed to the ATP-binding cassette (ABC) transporter proteins, located in the melanosomal membrane which actively pump toxic substances into the melanosomes for neutralization and thus reduce the effectiveness of the treatment [34,47]. This subcellular localization and conservation of organellar membrane integrity is therefore important as leakage of the cytosolic constituent into the extracellular space upon necrotic cell death activation (upon-plasma membrane damage), can result in a robust anti-tumour immune response[46,49,50]. In apoptosis, these cytosolic constituents will be sequestered by intact membranes of apoptotic cells, which are phagocytosed by surrounding macrophages [51,52]. Lastly, studies on mice showed that PDT may induce tumour-associated vasculature damage, which prevent metastases and subsequent tumour regression[53,54]. In order to improve PDT treatment in melanoma, several parameters aimed at overcoming resistance will necessitate further investigation. These may include: interventions which can temporarily reduce the amount or the pigmentation status of melanoma; the discovery of highly active PS absorbing in the 700–800-nm near infrared spectral region; immunotherapy approaches that can take advantage of the ability of PDT to activate the host immune system to the treated tumour, use of compounds that can reverse or inhibit drug-efflux of PS and finally combining PDT with other therapies such as chemotherapy.

1.3. HYPERICIN:

The success of PDT is related to the photosensitizer, presence of oxygen in the immediate environment and the induction of ROS through an appropriate photoactivation at a specific wavelength of light. In this study, we used hypericin, a natural photosensitizer, biosynthesised within the dark glands of the petals and leaves of the St John's Wort plant (*Hypericum perforatum*) (Figure 3A&B) [55,56]. It belongs to the chemical class of naphtodianthrones (Figure 3 C) and can be chemically synthesized through conversion of emodin to hypericin using Hyp-1 enzyme, yielding approximately 84.6% efficient conversion when overexpressed in E.*coli*[57,58]. This is a favourable alternative, as direct extraction from *H.perforatum*, produces a low yield of hypericin due to the low occurrence of the naphtodianthrones (0.05-0.3%)[59], which is costly and necessitates multiple cycles for purification, while requiring fast handling of materials[58]. Hypericin absorbs in both 300-400nm (ultraviolet) (Figure 3D) and 500- 600nm (white light)[60] range, with an optimal absorption peak at 563nm and emission at 600nm (Figure 3D)[61]. However, its

photosensitizing effect was discovered, when grazing animal feeding on the plants, developed non-desirous photosensitization of the skin upon sunlight exposure, through a biological reaction called hypericism [56].

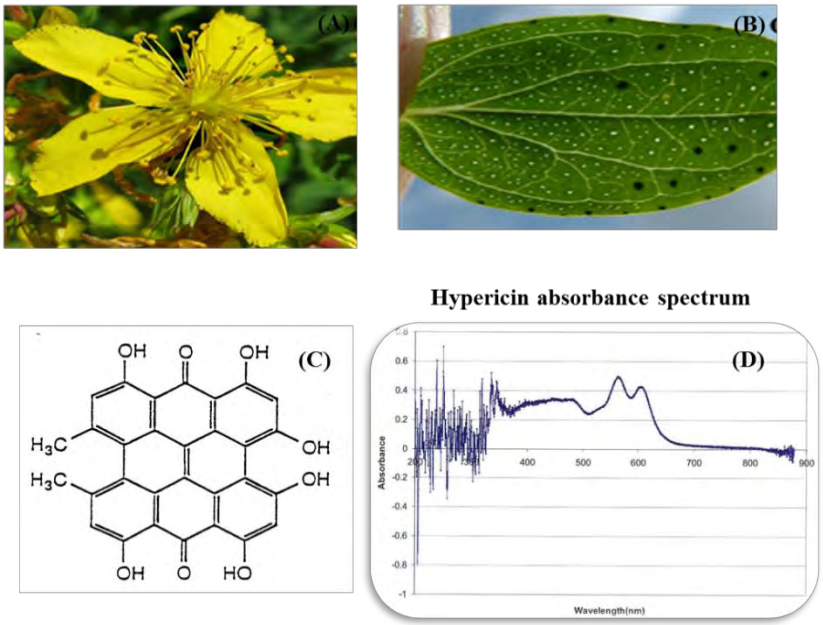

Figure 3: St John's Wort (*Hypericum perforatum.)*

(A)Hypericum perforatum plant and its (B) dark glands found in the leaves and petals, which (C) Hypericin's chemical structure, (D) hypericin absorbance spectrum (Internet source).

In humans, hypericin has been used for the treatment of various conditions including depression, anxiety, restlessness and sleeping disorders[62,63]. Moreover, its fluorescent properties have enabled the visualization of malignant tumour such as gliomas in a process known as photodiagnosis[64]. In addition, its photosensitizing properties have been widely used in treating several cancers (GH4C1 rat adenoma and human P3 squamous carcinoma cells)[65,66,67]. Hypericin has desirable properties as a photosensitizer, since it is not cytotoxic in the dark; has a low photobleaching, intense absorption spectrum in the visible light region, large excitation range and is rapidly cleared from the body while being preferentially retained within the tumour[68,69,70,71]. Due to its hydrophobic nature, hypericin is mainly absorbed within tumours cells through passive diffusion or by forming complex with the low-density-lipoproteins (LDL), which is overexpressed in the majority of cancer cells[56,70,72,].

During photodynamic treatment, hypericin mainly exercises its cytotoxic effect through production of singlet oxygen ($^1O_2$)[73,74], superoxide anion along with other ROS. In addition, production of ROS by hypericin has been shown to induce cell death through mechanisms such as apoptosis, necrosis and autophagy [42, 68,75,76,77]. This has been reported to be due to hypericin's subcellular localization upon PDT treatment[36,37,42,78]. Kessel and colleagues (1997)[79] found that localisation of etiopurpurin (PS) within the mitochondria and lysosomes resulted in a rapid apoptotic response. This was opposed to its analogue where a delayed apoptosis was observed due to its partial membranous localization, which promoted predisposition for necrotic cell death[79]. Other studies however reported on resistance to hypericin PDT treatment in melanoma and adenocarcinoma treatment[26,27,33]. In order to circumvent this HYP-PDT resistance, several attempts have been made, combining HYP-PDT with chemotherapeutic drug such as temozolomide (an analogue of dacarbazine), where it has been shown to increase tumour inhibitory growth potential on glioblastoma cells[80].This combined therapy, did not only improve the efficacy of the treatment, but also lowered the dose of the chemotherapeutic drugs, which resulted in reduced side effects. This study was confirmed by another group, which also found that combining chemotherapy and photodynamic therapy was more effective at killing human melanoma cells. However, this was achieved, through the use of the photosensitizing property of a mitoxantrone chemotherapeutic drug, resulting in lower light intensity[29]. In order to establish such a combination for treating the deadly disease that is melanoma, one would have to be selective in combining the hypericin with a good chemotherapeutic drug, which has currently been shown to be effective at treating melanoma. For this reason, this project chose the alkylating agent, dacarbazine.

1.4. DACARBAZINE (DTIC) AND MELANOMA

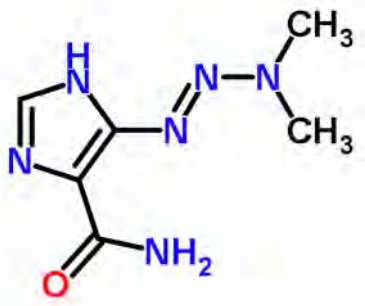

Figure 4: Dacarbazine chemical structure.

Dacarbazine (DTIC) is the only chemotherapeutic drug approved since 1975 (Figure 4), by the Food and Drug Administration (FDA) for the treatment of malignant melanoma[14]. DTIC is an alkylating agent, which exercises its cytotoxic effect by adding an alkyl group to DNA, thus causing DNA lesion formations, halting DNA synthesis and resulting in cell growth arrest and cell death[81,82]. During this process it is administered as a prodrug cytotoxic agent (DTIC), which has alkylating activity, resulting in generation of methyl DNA lesions inducing cell death.[83,84,85]. In melanoma, among the numerous methyl DNA lesions caused by DTIC, the most cytotoxic is the *0*-6-methylguanine (*0*-6-meG) [83,86]. These cytotoxic lesions (*0*-6-meG) can be repaired by *0*-6-methylguanine-DNA-methyltransferase (MGMT), which may affect DTIC efficacy when overexpressed in cancer cells[86,87]. From this observation, it might be implied that DTIC efficacy may rely on low MGMT repair and high activity of mismatches repair enzymes as it has been shown in melanoma[83].

Clinically, DTIC is mostly administered intravenously with a dose of 150 to 200mg/m^2 over five days[14]. However, single dose administration of 800 to 1000 mg/m^2 repeated every 3 to 4 weeks, is more suitable and well tolerated by patients[14]. Using this regime, a 15.3% objective response rate was achieved, in trials involving 1390 patients. Amongst this, 4.2% had a complete response as opposed to the remaining 11.1% where partial response was observed[14]. To date it's been the most effective chemotherapeutic drug in melanoma treatment, since it has shown superiority in patient survival, when compared to other treatment regimens in phase III trials[14,88]. Recently, Hervieu and colleagues (2013) showed in an in vivo experiment

that DTIC may induce tumour destruction by local activation of natural killer (NK) and T cells in melanoma[89]. However, the problem of chemoresistance remains. In order to overcome this chemoresistance, Kamila and colleagues (2013) showed that combining DTIC and parthenolide, resulted in a synergistic-inducing cell cycle arrest and apoptosis[82]. Moreover, this combination apart from reducing the number of viable cells, led to the eradication of the self-renewing capacity (clonogenic activity) of the melanoma cells, which DITC could not abrogate when used alone. Furthermore, when used alone DTIC (apart from being less effective on heterogeneous melanoma when compared to A375) induced increased secretion of vascular endothelial growth factor (VEGF), which promoted vascularisation favouring metastasis and relapse after treatment. However, in combination with parthenolide, the VEGF secretion was decreased, as well as its baseline level. Although this combination showed synergism, it however failed to reduce significantly the interleukin-8 expression (IL-8), whose overexpression has been shown to contribute to melanoma resistance to temozolomide treatment, a DTIC analogue[82,90]. Valero and colleagues (2010) also showed in an in vivo mouse model, that combining DTIC with dimethylfumarate; resulted in reduced lymph node metastasis[91]. Earlier, Thrall and colleagues (1991) showed that pre-treatment of murine melanoma cells with buthionine sulfoximine (50μM), reduced 90% of glutathione level (GSH) within the cells (which was fivefold higher in melanoma compared to melanocytes), causing an increased growth inhibitory effect on the cells[92]. Although these resistance mechanisms are crucial in improving DTIC treatment, other factors contributing to lower intracellular accumulation of DTIC below its cytotoxic threshold have been identified in melanoma[13,93]. This has been attributed to a family of ABC transporters, which are overexpressed in melanoma, and which upon DTIC treatment, is enriched in cells called a "side population". These cells have self-renewing capacity and the ability to grow under hypoxic conditions. Lastly, these cells have the potential to re-form the heterogeneous parental tumour, causing the relapse of treated patients observed clinically[93,94]. The study of these transporters therefore becomes pertinent with the aim of understanding chemoresistance.

1.5. MELANOMA THERAPY RESISTANCE AND ABC TRANSPORTERS

1.5.1. ABC transporters and chemoresistance

Speculation over what contributes to the cellular chemoresistance in melanoma has led to numerous theories. Of late, focus has shifted to the one feature that sets melanocytes and hence melanoma apart from other cell types, the melanosomes. These are membrane-bound organelles originating from the lysosomal lineage which seems to confer chemoresistance through a complex mechanism of drug trapping and export[95]. The central players in this mechanism are said to be the ATP-binding cassette (ABC) transporters which actively transport cytotoxic substances out of cells[96]. In humans, ABC transporters possess 48 genes, which are split into seven different subfamilies based on their domains and amino acid homology[97,98] (see Table 1). These transporters are ubiquitously expressed and located in cell membranes and multiple subcellular organelles (lysosomes, peroxisome, Golgi apparatus, mitochondria, endoplasmic reticulum), where they transport various molecules across the biological membranes in an ATP-dependent manner[5,96,99]. They can be categorized into two groups, consisting of the ABC "importers" mainly found in prokaryotes where they function to import nutrients within the cells and the eukaryotic ABC "exporters" whose function is tofacilitate the secretion of toxic compounds and various molecules out of the cells[99].

In humans however, each ABC transporter (exporter) contains a pair of ATP-binding domains referred to as a nucleotide binding fold (NBF) which is located within the cytoplasm and a pair of transmembrane domains (TM) embedded within the cell membrane (see Figure 5)[97,98].

Table 1: Overview of ABC transporters' expression profile in cell lines.

Transporter	Cell Line	Location	Expression	Drug	Reference
ABCB5	HEM; G3361; CDDP	7p24	Plasma membrane	none	[100]
ABCB1 (MDR1)	CS, H14, JR8	7p21	Cytoplasm	Doxorubicin	[100]
ABCC1 (MRP1)	CS, H14, JR8	16p13.1	Cytoplasm	Doxorubicin	[100]
ABCB8 (mABC1)	WM1552C; 451lu; WM793B	7q36	Inner mitochondrial membrane	Doxorubicin	[9]
ABCB5	WM2664 WM115; G361; A375; SKMEL28	7p24	Cell surface	Temolozide, DTIC; Doxorubicin	[13]
ABCB5	HEM; G3361; CD133	7p24	Cell surface and tissue	Doxorubicin	[101]
ABCG2 (MRP2) or (BCRP)	A375; G2; MRP1; HEK293; KB.V1	4q22	Cell surface	Vemurafenib	[102]
ABCG2	HaCaT	4q22	Not specified	Porphyrin	[103]
ABCG2	NCI.H1650; 1650 MX50; MCF7.TX200; MCF7.MX100; MCF7.VP	4q22	Cell membrane	Pyropheophrbid Chlorin 6; hematoporpyrin IX	[104]
ABCG2	RIF-1; Colo 26; BCC-1/KMC; HEK293; MCF7/MR; MCF7FLV1000; MF-10A	4q22	Cell Surface	Protoporphyrin X; (BPD-MA); imidazoacridino-ne; topotecan	[105,106]
ABCC1 (MRP1)	HT-29; HL60	16p13.1	Cell surface	hypericin	[33]
ABCG2 (BCRP)	HT-29; HL60	4q22	Cell surface	hypericin	[33]

During the efflux of cytotoxic molecules, a pair of ATP molecules bind to a portion of each NBF, which subsequently merges and undergoes a structural conformational change which results in ATP hydrolysis[98]. This ATP hydrolysis eventually leads to the release of energy, which is subsequently used to transfer the cytotoxic molecules (substrate) from the inner part of the membrane to the outer part through the two TMs (Figure 5)[98].

Recently, melanomas have been shown to express ABC transporters, which lower the intracellular accumulation of cytotoxic drugs [9,107]. Moreover, these transporters have been demonstrated to be highly expressed in highly tumorigenic subpopulations of melanoma and a number of groups have therefore suggested that they may be potential markers of melanoma stem cells[9,22,108,109]. One of these include the ABCB5 transporter, which seems to be characteristic of the resistant population and its expression results in therapeutic relapses, by re-forming the parental tumor along with a population of a more aggressive phenotype[110,111]. Additionally, in melanoma a population of cells overexpressing the ABCB5, ABCB1 and ABCB8 transporters, were found to be resistant to chemotherapeutic treatments with doxorubicin and dacarbazine[9,14,82,93,101,103,112]. Also, this ABCB5 and ABCB1 overexpression was found to correlate with cancer progression and aggressiveness.

Moreover, it has recently been reported that resistant populations overexpressing ABCB1/5 transporters have stem cell-like properties. These properties include self-renewal capacity (clonogenic capacity), spheres forming ability as well as yielding differentiated progeny and a population that can efflux dyes (reflective of the resistant population overexpressing the ABC transporter, which export dyes such as Rhodamine 123 or Hoechst)[93,110]. This is really important, since this resistant population has the ability to recapitulate the phenotype of the parental tumour, contributing to the heterogeneity of the tumour which can be associated with the relapse observed clinically[93,110]. Finally, reports have shown the ability of this resistant population to grow under aggravating condition such as hypoxia, through up-regulation of genes such as hypoxia-inducing factor 1α (HIF1α) under the influence of its upstream regulator, PI3K/AKT[93,110]. However, a report has shown that overexpression of transporters such as ABCC1 and ABCG2 in adenocarcinoma cancer reduced HYP-PDT killing efficiency, as well as other photosensitizers. [30, 103,113, ,114,]. This is of particular interest as, recent work in our lab has shown that the photosensitizer hypericin co-localizes with melanosomes involved in melanoma resistance to HYP-PDT. In order to combine the chemotherapeutic treatment with the possible adjunctive photodynamic therapy, one may have to investigate

what is the ABC transporter profile in resistance to this therapeutic treatment (PDT) in skin cancer.

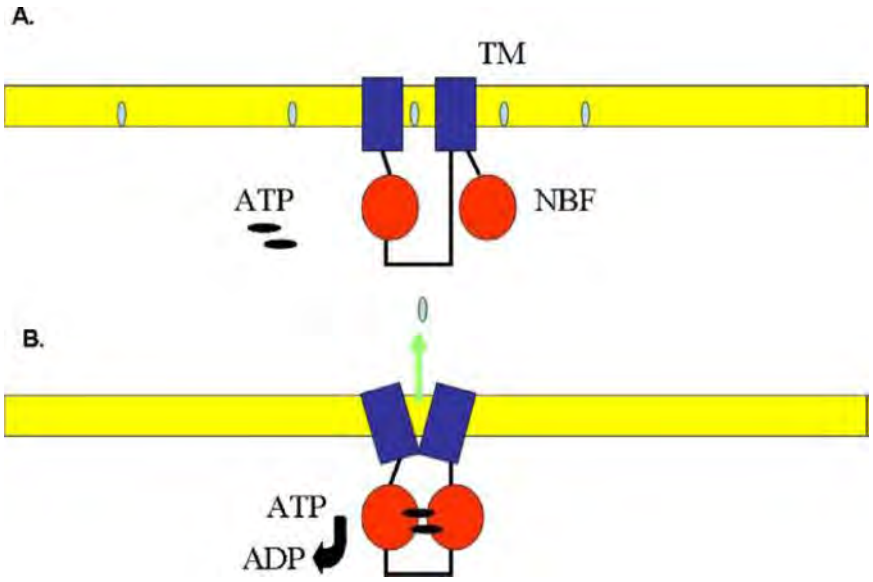

Figure 5: Diagram of an ABC transporter.
(A). A prototypical ABC transporter is shown with two sets of transmenbrane domains (TM, blue) and two nucleotide binding domains (NBF, red), free ATP molecules and substrate molecules in the inner membrane leaflet (light Blue). **(B)** Upon binding of ATP, the NBFs are joined, leading to a conformational change, and the movement of the substrate molecule[98].

1.5.2. ABC transporters and photodynamic therapy resistance

Photodynamic therapy has produced promising results in melanoma, however resistance soon developed as a result of ABCG2 transporter overexpression, which has shown to lead to an efflux of photosensitizers including: hypericin, pheophorbide a, pyropheophorbide a, chlorin e6, 5-aminolevulinic acid (5-ALA) and protoporphyrin IX [103,114,115 ,116].

The ABCG2 is a half transporter (consisting of one NBF and TM) and is a member of the heme efflux system, which becomes functional upon dimerization, and hence effluxes various molecules[103]. The importance and specificity of the ABCG2 transporter to efflux photosensitizers was emphasized in a recent study where it was shown that its inhibition with non-toxic Ko-134 (analogue of fumitremorgin C)[103], increased the efficacy of PDT in human keratinocytes (HaCat cells). This result was supported by Liu et al.(2007) who showed that inhibition of the ABCG2 transporters using imatinib mesylates, resulted in increased

intracellular accumulation of the PS (2-devinyl-pyropheophorbide a, protoporhyrin IX and benzoporphyrin derivative monoacid ring A) within basal cell carcinoma cells (BCC) (ABCG2 positive) and not within squamous cell carcinomas (ABCG2 negative). This increase of PS within the BCC, was correlating with increased phototoxicity and selectivity, resulting in tumour destruction[105].

A further aspect that contributes significantly to the therapeutic efficacy of a treatment modality such as PDT is the intracellular localization of the photosensitizers. The fact that ABC transporters are found localized in the subcellular membranes (mitochondria, lysosomes, peroxisomes, melanosomes and Golgi apparatus) mean that their roles in therapeutic resistance with respect to organellar localization cannot be underestimated and needs to be investigated. One example is their localization in melanocyte-specific organelles called melanosomes. These organelles house the process of melanogenesis and subsequent accumulation of the pigment melanin. The melanosomes are surrounded by a double membrane due to the toxic intermediates produced during the process of forming melanin. Our lab, and others have shown that pigmented melanoma was more resistant to HYP-PDT, when compared to unpigmented melanoma cells and suggested that this was partly due to the pigment melanin, as temporary removal of the melanin using Kojic acid, sensitized the cells to the HYP-PDT treatment[27]. This correlated with increased ROS, thus unveiling the scavenging property of the pigment melanin and mature melanosomes[27]. This differential sensitivity to PDT was further corroborated by both Sparsa et al. (2013) and Jend et al. (2009) who showed that the combination of the pigment melanin and up-regulation of ABCG2, caused resistance in colon cancer to HYP-PDT[113, 117.] Upon pre-treatment with proadifen (affecting ABCG2 function), this resistance was reversed due to increased intracellular level of HYP and ROS, which subsequently resulted in mitochondrial membrane damage and concomitant cell death[113]. A further study contributing to the hypothesis of ABC transporters expressed on subcellular organelle membranes being important to cancer treatment resistance, was published by Goler-Baron and Adar et al. (2012) who demonstrated that resistance in breast cancer was developed, when ABCG2-rich extracellular vesicles and lysosomes trapped the photosensitive drugs imidazoacridinone and topotecan (In breast cancer), thus preventing them from reaching their therapeutic targets[30,118]. Reversal of this resistance was achieved, upon illumination of these ABCG2-rich extracellular vesicles and the lysosomes containing the drugs, resulting into severe membranous damage, due to the production of ROS[30].

In summary, approaches to overcome the ABC transporters in skin cancer resistance to PDT are needed. One of these approaches could be combination therapy, as Jin-Chul and colleagues (2013) showed that combining Cisplatin to 5-ALA photodynamic therapy (both efflux by ABCG2), led to greater tumour destruction both in vitro and in vivo, when compared to individual treatments in squamous cell carcinoma[28]. This had the advantage of not only having greater tumour destruction, but also to lower the concentration of the chemotherapeutic drug (thus, lowering of side effects)[28]. Other treatments may involve pre-treatment of melanoma or non-melanoma skin cancer (NMSC) tumours with proadifen or verapamil (ABCG2 transporter inhibitor), and then performing HYP-PDT or pre-treating the cells with bafilomycin A1 to prevent lysosomal localization of the drugs followed by application of PDT treatment.

1.6. AIM OF THE STUDY:

Due to the heterogeneity of melanomas at a molecular and cellular level, and the paucity of information regarding their ABC transporters status, this study hypothesizes that chemoresistance is integrally related to the ABC transporter expression in these cells and that a synergistic action between DTIC and PDT can influence the chemoresistance properties of melanoma cells and thus render them more susceptible to cell death.

In order to realize the above aim, the following objectives were set out:

1) To establish the DTIC concentration killing fifty percent (LD_{50}) of pigmented and unpigmented metastatic human melanoma cell lines.

2) To investigate the cytotoxic effect of the combination of DTIC and HYP-PDT in the melanoma cell lines

3) To determine the protein expression of the ABC transporters in response to single (PDT only) and combination (PDT+DTIC) therapies.

4) To investigate the clonogenic potential of the pigmented and unpigmented melanoma cell lines after single and combination therapies.

Chapter 2: Materials and Methods

2.1. CELL CULTURE

For all experiments, human melanoma cell lines were used. The human A375, unpigmented melanoma cell lines were obtained from the American Type Culture Collection (ATCC, USA), while the pigmented, UCT-Mel-1 was originally isolated from the metastatic lymph node of a patient at Groote Schuur Hospital (GSH), Cape Town, South Africa. The HeLa cell line (Cervical cancer cell lines) was a generous gift from Prof.Virna Leaner, who obtained the cells from ATCC. However, the 293T cell line (Embryonic kidney cells) was generous gift from Prof.Susan Kidson laboratory. All the cell lines, were grown in Dulbecco's Modified Eagle's Medium (DMEM, Highveld Biological (Pty) Ltd., RSA), supplemented with 10% (v/v) heat inactivated foetal bovine serum (Highveld Biological (Pty) Ltd., RSA), 100U/ml penicillin (P3032 Sigma, USA) and 100µg/ml streptomycin (S-91370 Sigma, USA), and incubated in 5% $C0_2$, 95% humidity at 37^{o}C (See appendix A, B & C).

2.2. DACARBAZINE (DTIC) TREATMENT

Dacarbazine (DTIC) was obtained from Sigma, South Africa (D2390). DTIC was diluted to a working stock of 10mM in NaCl (0.9%), from the original stock solution and stored as aliquots at -20 ^{o}C. From these aliquots, concentrations ranging from 0.480mM to 3mM were used and subsequently diluted in the cell culture medium, for each experiment. The final concentration of NaCl in all experiments remained equal or less than 0.9%. Human UCT-Mel1 and A375 cells were seeded into 96-well tissue culture grade plates (Greiner CELLSTAR, South Africa) and allowed to adhere overnight at 37^{o}C in a 5% $C0_2$ humidified incubator (MCO-175M, Sanyo). The following day, the medium was removed and the cells were exposed to DTIC concentrations of 0.480, 0.850, 1, 1.5 and 3mM, for a further 24 and 48hours at 37^{o}C. After the treatment, a cell viability assay was conducted to assess the cytotoxic effect of DTIC on the cells.

2.3. CELL VIABILITY ASSAY

Cell viability following DTIC treatment was monitored using the XTT assay according to manufacturer instructions (XTT Cell proliferation Kit II Cat. No 11465015001, Roche, Germany). Briefly, this was performed by adding XTT solution, four hours prior the end of

the 24 or 48 hours DTIC treatment period. In this assay metabolically active cells cleave the yellow tetrazolium salt, to form orange formazan crystals, which absorb light at 450nm and 650nm (reference wavelength), using a spectrophotometer (Versamax, Molecular devices, South Africa), using softMax pro4.3.1 software. The absorbance values were normalized to the untreated control (vehicle) and results presented as percentage of cell viability.

2.4. HYPERICIN

Hypericin from the *Hypericum perforatum species*, (95% pure by high-performance liquid chromatography), was obtained from Sigma, South Africa (56690). A 2mM stock solution (Appendix D) was made in dimethyl sulfoxide (DMSO, Merck) and stored as aliquots at -80°C. Working solutions were prepared fresh at a concentration of 50µM in phosphate-buffered saline (1x PBS, Appendix E) and then diluted further directly in the complete cell culture medium containing fetal bovine serum (Appendix A& B). All experiments were carried out under subdued light conditions.

2.5. LIGHT ACTIVATION

Hypericin was activated with 5J/cm^2 using green-yellow laser light (Fiber coupled laser nodule, 561nm, RGBlase LLC, California, USA). A light with fiber optic cable (561nm) was used to administer the dose. The power output was measured to 20mW using a portable power meter (FieldMate, Laser Power Meter). The following equation was used to obtain the time of exposure.

$$Time = \frac{Dose\ (J/cm^2))}{Power\ Density\ (W/cm^2)}$$

2.6. HYPERICIN-PHOTODYNAMIC THERAPY (HYP-PDT)

UCT-Mel1 and A375 cells were exposed to 4 hours of hypericin in complete media followed by a wash in, 1xPBS and light activation with 5 J/cm^2 yellow-green laser in 1x PBS for all experiments. Following light activation, complete media was added to the cells. At different times after treatment (24 and 48 hours) the cells were subjected to various analyses.

2.7. COMBINATION THERAPY: DACARBAZINE +HYP-PDT

UCT-Mel1 and A375 cells were seeded into 35mm dishes (Irradiated and unirradiated plates, having control/vehicle and treated wells), and left overnight at 37^{o}C to adhere. The following day, the cells were treated with a DTIC concentration (1250µM) for 24 or 48hours. Four hours before the end of the DTIC treatment time points (i.e. 20 and 44h), the cells were exposed to 3µM hypericin for 4 hours, followed by two successive washes in 1x Phosphate buffer Saline (PBS). Upon completion of the HYP-PDT (performed in 1xPBS), which was performed at 20mW with a light intensity of 5J/Cm^2, the 1xPBS was gently removed and new medium was replaced. The cells were then subjected to additional analyses. For each experiment cells were exposed to ten different treatments:

- vehicle with no-irradiation (V-L)
- vehicle with light-activation (V+L)
- Control with no-irradiation (C-L)
- Control with light-activation (C +L)
- DTIC with no-irradiation (DTIC-L)
- DTIC with light-activation (DTIC +L)
- hypericin with no-irradiation (HYP-L)
- hypericin with light-activation (HYP+L)
- hypericin+DTIC with no-irradiation (HYP+DTIC-L)
- hypericin+DTIC with irradiation (HYP+DTIC+L)

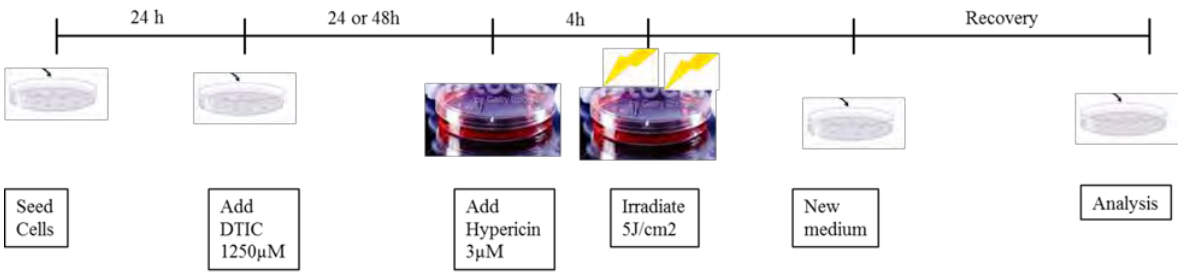

Figure 1: Experimental set up for combination therapy. Melanoma Cells were seeded and left to adhere to the dish overnight. The following day, the cells were exposed to DTIC (1.25µM) for 24 or 48h. Thereafter, the cells were exposed to hypericin for 4 hours (prior the end of DTIC treatment) followed by light activation with 5J/cm^2 at a power of 20mW (49seconds per well within the 96 well plate and 40min for each 35mm dish). Upon completion of the treatments, the cells were put in new medium and left for 24h recovery, before further analysis were performed.

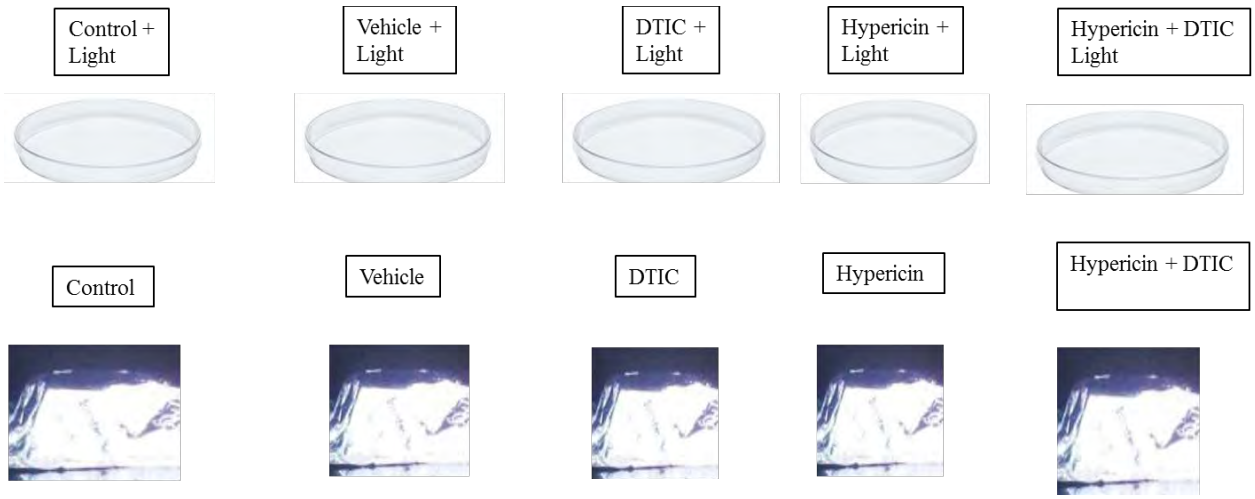

Figure 2: The different treatments of the combination therapy (DTIC+HYP-PDT).

2.8. WESTERN BLOT ANALYSES: ATP-BINDING CASSETTE (ABC) TRANSPORTER PROTEIN EXPRESSION

Western blot analysis is an indirect method used to detect proteins of interest by resolving the sample protein on polyacrylamide gels, followed by the electrophoretic transfer of the protein onto membranes. This is followed by detection using specific antibodies to the protein(s) of interest followed by enhanced chemiluminescence (ECL) detection (Thermo scientific, Prod# 34080, USA) on an x-ray film (SANTA CRUZ biotechnology, catalog# sc-201697, USA)

For the preparation of cell lysates, UCT-Mel1 and A375 cells were grown to 70% confluency and treated with 1250µM DTIC alone or with combination therapy (DTIC+PDT). After the experimental period (24 hours), adherent cells were harvested and proteins were extracted on ice by adding complete radio-immunoprecipitation assay (RIPA) buffer (Appendix I&J) to the dish of cells. Cells were collected with a cell scraper and the lysed cells were then transferred to a 1.5 ml microfuge tube, vortexed and shaked on ice, for 30 min on the belly dancer (STOVALL, life science, inc, Greensboro, NC USA). Samples were then centrifuged at 12000 rpm at 4^{o}C for 20 min. The supernatant was finally transferred to a clean 1.5 ml microfuge tube and stored at -80^{o}C till further analyses were conducted.

The protein concentration of the samples was determined using the Pierce BCA Protein Assay Kit (Thermo Scientific, USA). This kit is a colorimetric assay where a purple coloured reaction product is produced upon chelating reaction between two bicinchoninic acid molecules and one cuprous ion. This product is then read spectrophotometrically (Versamax Tunable microplate reader-molecular devices, South Africa) at 562 nm and compared to a standard curve generated using known concentrations of bovine serum albumin (BSA, Sigma-Aldrich, USA) . The protein concentration of each sample was then calculated using SoftMax Pro software (Version 4.3.1 Life Sciences Edition, USA).

To analyse protein expression, identical amounts of proteins (30µg), were diluted in 5x loading dye, loaded into wells of stacking and resolving SDS-polyacrylamide gel (7.5/ 5%) and electrophoresed at 80V for 30min and 120 V for 1hour in 1x running buffer. The separated proteins were then transferred, at 100V for 1hour, onto a nitrocellulose membrane (Hybond ECL Amersham, RPN203D, GE Healthcare), in 1x transfer buffer. The blotted membrane was subsequently immersed in Ponceau-S and stained for total protein for 5min. The membrane was then briefly washed in water, and digitally scanned (CanoScan LiDE210, Canon). The membrane was doubly immersed in 1x TBS-T for 5min, before being blocked for 1hour at room temperature in 5% milk TBS-T. Upon blocking completion, the membrane was exposed to the primary antibodies (ABCB1/5 & ABCG2 (1:200), p38 (1:5000)) overnight at 4 ^{o}C. The following day, the membrane was washed (3x 10min) in 1x TBS-T and the secondary antibodies (Goat-anti mouse (1:1000)/ (1:3000) & donkey-anti Goat (1:4000)/ (1:3000) and Goat-anti rabbit (1:5000)) were added for 1hour at room temperature (see table 1) and exposed to SuperSignal West Pico chemiluminescent ECL detection reagent

for 1min. Finally for immunodetection, the X-ray film, was manually exposed to the membrane developed (G150, AGFA) and fixed (G354, AGFA) for viewing.

2.9. MICROGRAPHY OF COMBINATION THERAPY (DACARBAZINE+HYP-PDT)

UCT-Mel1 and A375 metastatic melanoma cells were seeded in 35 mm^2 coverslips in 35mm^2 cell culture dishes (200 000) and treated according to the laser induced DTIC+HYP-PDT treatment protocol (see Figure 1), for 40min with light intensity of 5J/Cm^2 at a power of 20mW. Once the treatment was completed, the cell's nucleus were stained for 30min, through addition of the nuclear Hoechst dye (33342/33258) (10mg/ml) to the medium at a dilution of 1:5000. Upon completion of the nuclear staining, the medium was removed (DMEM++) and replaced with a serum free medium (DMEM). The cells were then viewed immediately with a fluorescent microscope (Carl Zeiss, Axiovert 200M, (Germany) at a magnification of 400X, using the coverslips. Images were recorded with appropriated digital software (AxioVision V.SPI) in the blue (Hoechst) and Cy3 (HYP) channels. Overlay pictures of these 2 channels, as well as their respective phase contrast images were also captured. Scale bars of 50µM were included on each picture.

2.10. CLONOGENIC ASSAYS

The clonogenic capacity of the UCT-Mel1 and A375 metastatic melanoma cells, upon combination (DTIC+HYP-PDT) and chemotherapeutic treatments was investigated. This was performed, by seeding melanoma cells into 6cm dishes and leaving them overnight at 37^0C for adherence. The following day, the cells were treated with DTIC alone or with combination therapy (DTIC + HYP-PDT) for 24 hour. Upon treatment completion, the cells were lifted using trypsin/EDTA (See appendix F), counted and re-plated to a lower density (400 cells per well) into 6 well plates. Once enough colonies were formed from the re-plated cells, medium was removed from each well. Then, the cell colonies were fixed with (3:1) methanol: acetic acid, for 15min per well after which each well was stained with 0.5% crystal violet in methanol for 15min, rinsed with ethanol and prepared for micrography.

Pictures were analysed using Image J software (version 1.43u; National Institutes of Health, USA).

2.11. STATISTICS

Different statistical analyses were performed on the data obtained depending on the type of experiment performed. For cell viability and colonogenic assay of UCT-Mel1 and A375 upon chemotherapy and combination therapy (DTIC+HYP-PDT), a 1way ANOVA and Bonferroni's/Dunnett's multiple comparisons post-test were applied to the results. However, for densitometry analysis of the western blot results and clonogenic assay, a T-test was performed. A P-values of <0.05 was considered to be of significance. All graphs and statistics were performed using GraphPad Prism (Version 5.01, USA).

Table1: concentrations of primary and secondary antibodies used

Primary antibody (in 5% fat-free milk-TBS-T)	**Conc.**	**Secondary antibody**	**Conc.**
ABCB5 (Cat: (N-13):sc-104019, Goat polyclonal, Santa Cruz Biotechnology, USA)	1:200	Donkey anti-goat Horseradish peroxidase conjugated (Cat: sc-2020, Santa Cruz Biotechnology,USA)	1:4000 in 5% fat-free milk-TBS-T
Mdr-1 (Cat: (D-11):sc-55510, mouse monoclonal, Santa Cruz Biotechnology, USA)	1:200	Goat anti-mouse Horseradish peroxidase conjugate (Cat: 170-6516, BioRad Laboratories,USA)	1:3000 in 5% fat-free milk-TBS-T
ABCG2 (Cat: (6D-171):sc-69988, mouse monoclonal, Santa Cruz Biotechnology, USA)	1:200	Goat anti-mouse Horseradish peroxidase conjugate (Cat: 170-6516, BioRad Laboratories,USA)	1:3000 in 5% fat-free milk-TBS-T
p38 (Cat: p-38 MAP Kinase: MO800 rabbit polyclonal, Sigma-Aldrich, Germany)	1:5000	Goat anti-rabbit Horseradish peroxidase conjugate (Cat: 170-6515, BioRad Laboratories,USA)	1:5000 in 5% fat-free milk-TBS-T

Chapter 3: Results

3.1. CELL VIABILITY OF HUMAN METASTATIC MELANOMA FOLLOWING DACARBAZINE TREATMENT (24 AND 48 HOURS)

Investigating the possible synergistic action of chemotherapy (DTIC) and hypericin activated photodynamic therapy (HYP-PDT) in resistant melanoma skin cancer was the central aim of this project. In order to realise it, the lethal dose of the chemotherapeutic drug DTIC killing 50% of metastatic melanoma cells (LD_{50}), had to be established before combining it with HYP-PDT. As displayed in figure 6, both pigmented (UCT-Mel1, Figure 6A) and unpigmented (A375, Figure 6B) metastatic melanoma were treated with increasing DTIC concentrations ranging from 0.48 to 3mM. After 24 hour treatment, cell viability, which was normalised to the vehicle control (0.9% NaCl), revealed that none of the DTIC concentrations were cytotoxic to the pigmented UCT-Mel1 melanoma (Figure 6A). In contrast, 1.5mM DTIC significantly reduced the viability of the A375 melanoma cells but this decrease was only 20% less than the control (Figure 6B). Unexpectedly, 3mM had no effect on the viability of A375 melanoma cells. These results prompted the extension of the DTIC treatment for an additional 24 hours to an overall 48hour treatment.

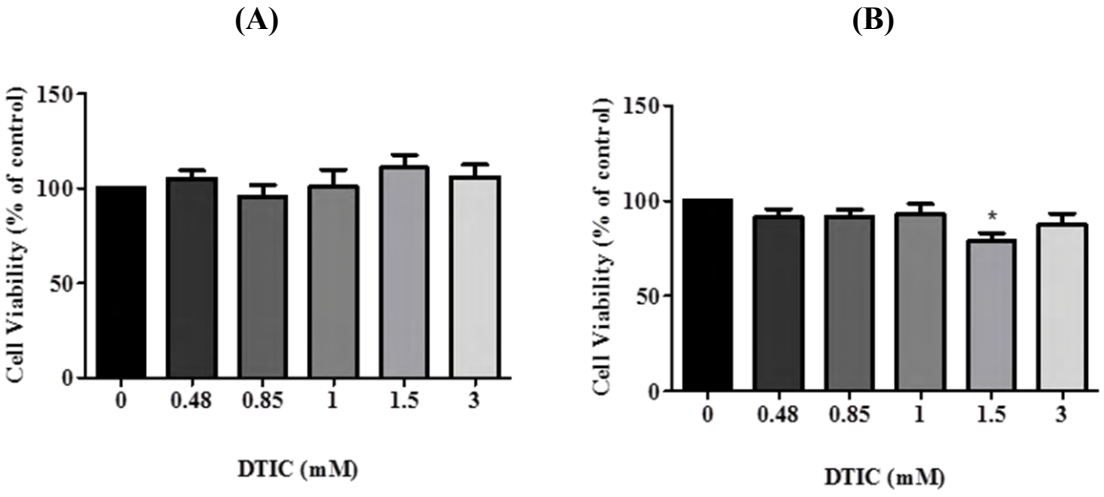

Figure 6: Cell viability 24 hours post DTIC treatment of pigmented (UCT-Mel1) and unpigmented (A375) human metastatic melanoma cell lines. UCT-Mel1 (A) and A375 (B) melanoma cells were treated with various DTIC concentrations (0.48; 0.85; 1; 1.5 and 3mM) for 24 hours. Following treatment, cell viability was analyzed using the XTT assay. Results were presented

as percentage of cell viability normalized to the 0.9% NaCl control. Significant difference = P *< 0.05. Statistical analysis used 1way ANOVA and Dunnett's multiple comparison test; n=3).

Upon completion of the 48hour DTIC treatment, a significant 22.3% reduction in cell viability could be seen in the UCT-Mel1 (pigmented) melanoma cell line treated with 1.5mM DTIC (Figure 7A). Interestingly, in the unpigmented A375 (unpigmented) melanoma, a significant dose-dependent decreased in cell viability could be observed for all the tested concentrations resulting in an LD_{50} of 1.25mM (figure 7B). These results suggested that UCT-Mel1 (pigmented) was more resistant to the DTIC treatment, when compared to the A375 (unpigmented) cells at all treated concentrations.

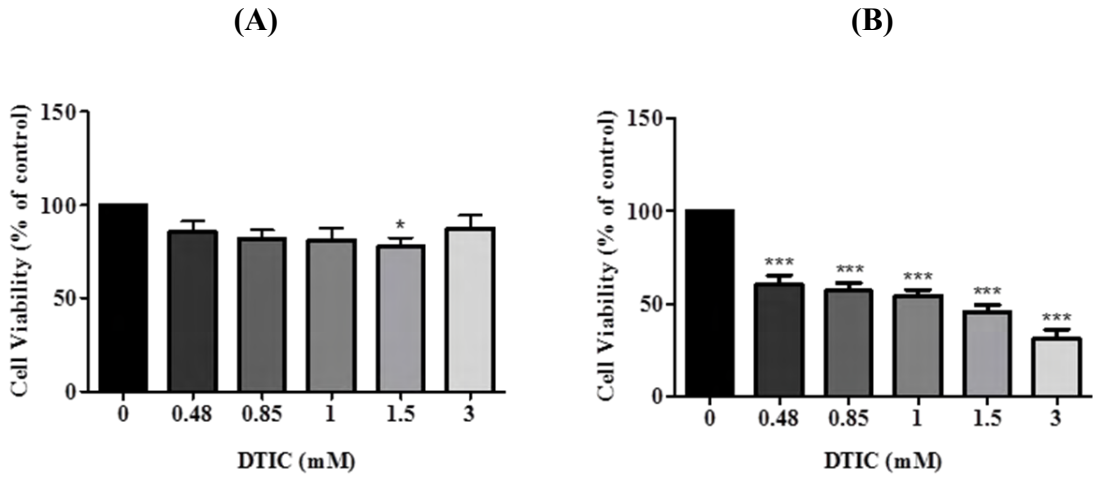

Figure 7: Cell viability 48 hours post DTIC treatment of pigmented (UCT-Mel1) and unpigmented (A375) human metastatic melanoma cell lines. UCT-Mel1 (A) and A375 (B) melanoma cells were treated with various DTIC concentrations (0.48; 0.85; 1; 1.5 and 3mM) for 48 hours. Following treatment, cell viability was analyzed using the XTT assay. Results were presented as percentage of cell viability normalized to the 0.9% NaCl control. Significant difference = P *< 0.05, ***<0.0001. Statistical analysis used 1way ANOVA and Dunnett's multiple comparison test.; n=3.

3.2. CELL VIABILITY OF HUMAN METASTATIC MELANOMA FOLLOWING COMBINATION THERAPY TREATMENT (DTIC+HYP-PDT) AT 24 AND 48 HOURS

Recent work in our lab showed that 3μM activated HYP-PDT was lethal to both pigmented (UCT-Mel1) and unpigmented (A375) metastatic melanoma cell lines 24hours post-treatment. Hence, this concentration of HYP was then used in combination with the DTIC lethal dose causing fifty percent decrease in unpigmented melanoma cell viability (LD_{50}, 1250μM).

As depicted in figure 8A (DTIC+L), the UCT-Mel1 cells displayed an expected 3.6% decrease in cell viability upon exposure to DTIC. Interestingly, a significant reduction of 50.19% occurred with activated hypericin-PDT (Fig 8A, HYP+L). Despite the combination therapy (Fig 8A, DTIC+HYP+L) causing a reduction of 61.26% in the UCT-Mel1's, this was not significantly different to the HYP-PDT alone (HYP+L). This suggested no additive combinatorial effect in the pigmented melanomas at 24hours. At the 48h time point (Fig 8B) however, the picture was quite different with the combination therapy (Fig 8B, DTIC+HYP+L) reflecting a significant difference (DTIC+L vs DTIC+HYP+L, $p<0.001$) between the chemotherapy alone and the combination treatment. This result suggests that a later time point enhances the combination efficacy (77.75% reduction in cell viability Fig 8B, DTIC+HYP+L) in highly resistant pigmented melanomas. Taken all together, these experiments had shown that HYP-PDT (Hypericin activated photodynamic therapy) and DTIC+HYP+L (combination therapy), were definitely overcoming the resistance observed after chemotherapeutic (DTIC) treatment at 24hours. Moreover, it also showed that the cytotoxicity observed within the DTIC+HYP+L was not a result of synergism, as this was not significantly different to the HYP+L group (Figure 8A& 8B).

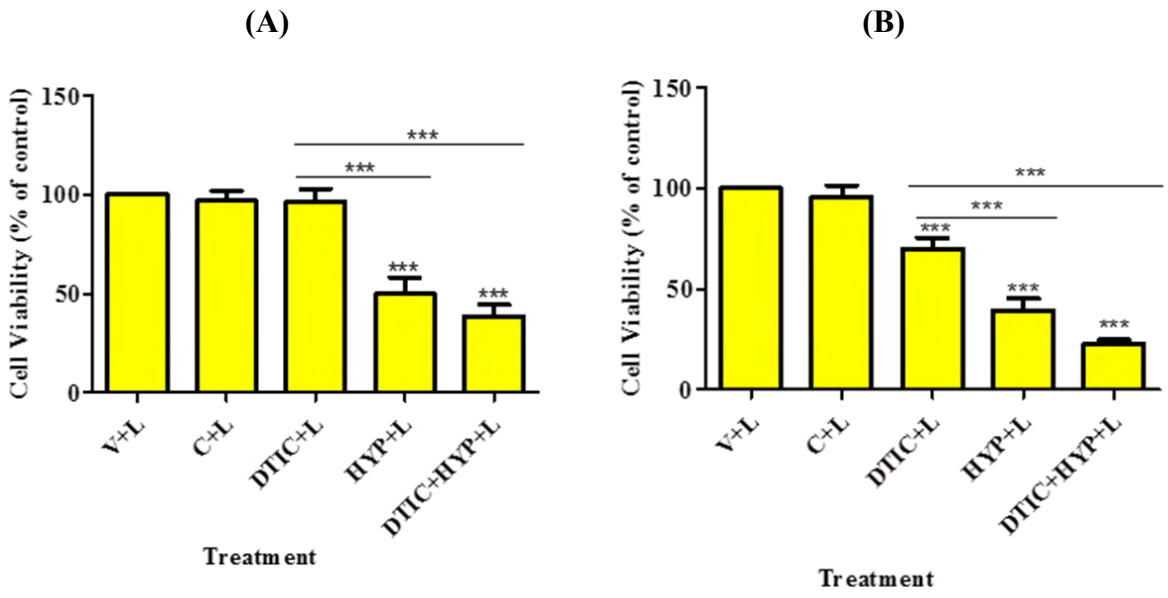

Figure 8: Cell viability 24 and 48 hours post combination therapy using 1250µM DTIC and 3µM HYP-PDT on UCT-Mel1 (pigmented) human metastatic melanoma cells. UCT-Mel1 cells that were sequentially exposed to DTIC and irradiated with HYP (exposed to laser light) at 24 and 48hour (A) and (B). Statistical difference = * < 0.05, **<0.001 and ***<0.0001. Statistics was analysed using a 1 Way ANOVA and Bonferroni's multiple comparison test. n=3.

Analysis from the A375 treated group have shown that, depending on the respective therapy used i.e. chemotherapy and/or PDT, there was a decrease in cell viability characterised by a reduction of 25% (DTIC), 55.1% (HYP+L) and 65.7% (DTIC+HYP+L) when compared to their vehicle control (0.9% NaCl + 0.15% DMSO) (Figure 9A). Although, HYP+L and DTIC+HYP+L were significantly different to their control (Figure 9A, P<0.0001), they were not significantly different to each other. However, (HYP+L and DTIC+HYP+L) were significantly different to the DTIC treatment only (Figure 9A, P<0.05 & P<0.0001). At 48 hours (Figure 9B), a decrease in cell viability could be observed within the irradiated group (Figure 9B). The reduction was characterised by 50, 66 and 83.2% reduction in cell viability for DTIC+L, HYP+L and DTIC+HYP+L treatment, respectively (Figure 9B). However, significant differences were only obtained with DTIC+L, compared to the DTIC+HYP+L treatment (Figure 9B, P<0.001). Activated HYP (Figure 9B, HYP+L) showed no significant difference to the combination treatment (DTIC+HYP+L). Moreover, a reduction in cell viability could be seen, when the untreated A375 melanoma cells were compared to their vehicle control (Figure 9B, V+L). However, after 48h of treatment in the unirradiated group (Figure 9C), all the treated groups showed a significant reduction in cell viability (50, 18.4 and 59% upon DTIC-L, HYP-L and DTIC+HYP-L treatment, respectively). This further

emphasises that a longer period of exposure leads to a more potent effect even in the absence of light activation. In conclusion it could be deduced that PDT, chemotherapy (DTIC) and the combination thereof are more efficient at killing A375 unpigmented melanoma cells, as opposed to their more resistant pigmented UCT-Mel1 counterparts (Figure 6, 7,8 and 9).

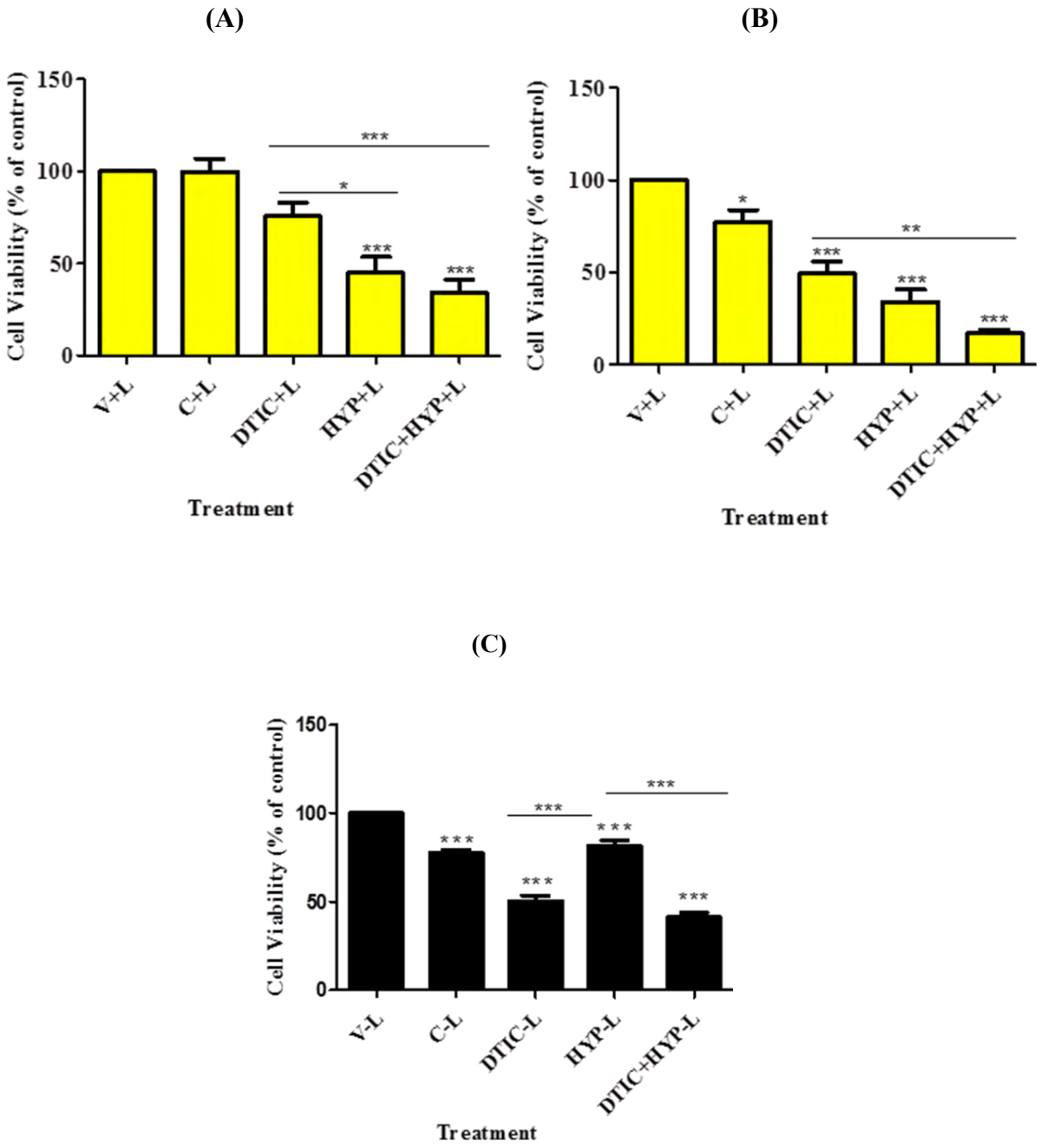

Figure 9: Cell viability 24 and 48 hours post combination therapy using 1250µM DTIC and 3µM HYP-PDT on A375 (unpigmented) human metastatic melanoma cells. A375 cells that were sequentially exposed to DTIC and irradiated with HYP (exposed to laser light) at 24 and 48hour (A) and (B); A375 cells which were unirradiated at 48hour (C) .Following treatment, cell viability was

performed using the XTT assay and data was normalized to the 0.9% NaCl control. (Statistical difference = * < 0.05, **<0.001 and ***<0.0001. Statistics was analysed using a 1 Way ANOVA and Bonferroni's multiple comparison test. n=3).

3.3. METASTATIC MELANOMA CELL MORPHOLOGY 24 HOURS POST THERAPEUTIC TREATMENTS

Following the determination of the cytotoxicity of the different treatments on the melanoma cells, the next objective was to investigate the morphological changes associated with these therapies 24 hours post-treatment.

As displayed by the phase contrast image (Figure 10A) untreated A375 melanoma cell lines displayed a non-dendritic triangular, cobblestone-like morphology, upon confluence. However, when A375 cell lines were treated with DTIC for 24hours an alteration in cell morphology was observed. The treated cells now displayed irregular cell borders, with enlargement of their cytoplasm and a distinct flattening of the cells, gradually losing the triangular morphology (Figure 10B).

(A) **(B)**

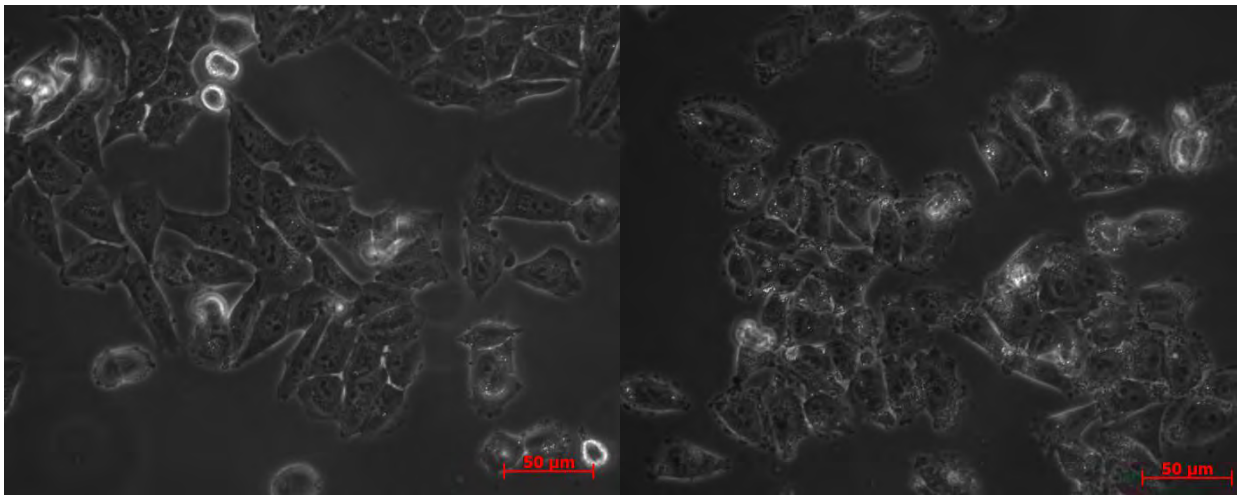

Figure 10: Phase contrast images of unpigmented A375 melanoma cells (A) and dacarbazine (DTIC) treated A375 cells (B). A375 cells were cultured and treated with 1250 µM DTIC for 24hour. Images were captured 24 hour post-treatment. Magnification: 400x; Scale bar = 50µM.

Moreover, an increase in cell size could be observed with cells exposed to inactivated hypericin (HYP-L) for 24 hours. A number of these cells also displayed irregular membrane borders (Figure 11A, arrows). The DTIC+HYP combination treatment further resulted in a swelling of the cells accompanied with cellular rounding up, irregular cytoplasm and progressive loss of membrane integrity and an associated decrease in confluence (Figure 11B).

(A) **(B)**

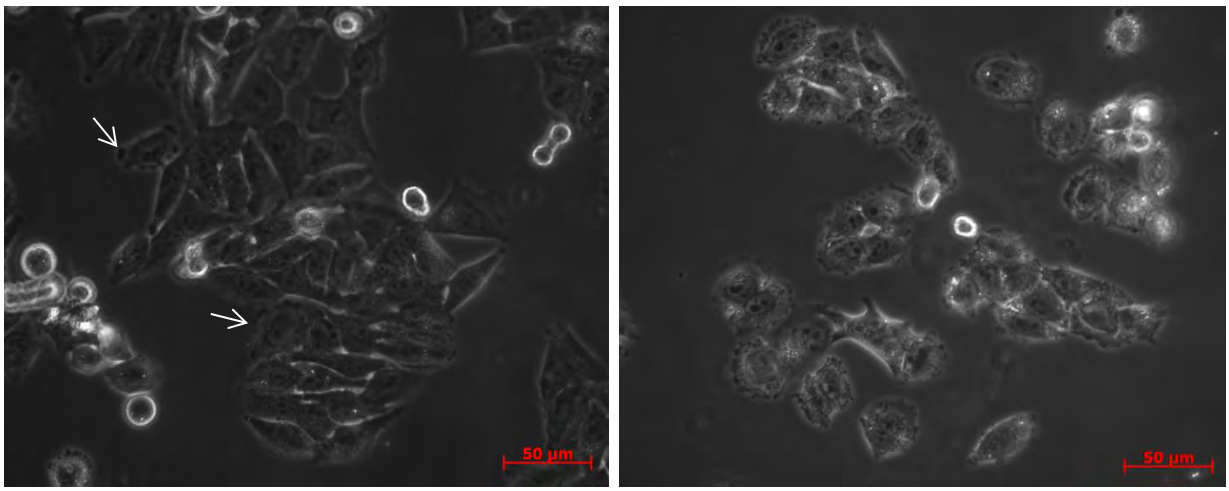

Figure 11: Phase contrast images of unpigmented A375 melanoma cells; 24hour post-inactivated hypericin (HYP-L) (A) and combination therapy treatment (DTIC+HYP-L) (B). A375 cells were either exposed to HYP only or to DTIC+HYP-L for 24 hour. Images were captured 24 hour post-treatment**.** Magnification: 400x; Scale bar = 50µM.

Starkly, both HYP-PDT and DTIC+HYP+L treatment resulted in cell size reduction, cell swelling and pronounced vacuolisation in the cytoplasm with increased granularity and cell shrinkage (Figure 12A & 12B).

(A) **(B)**

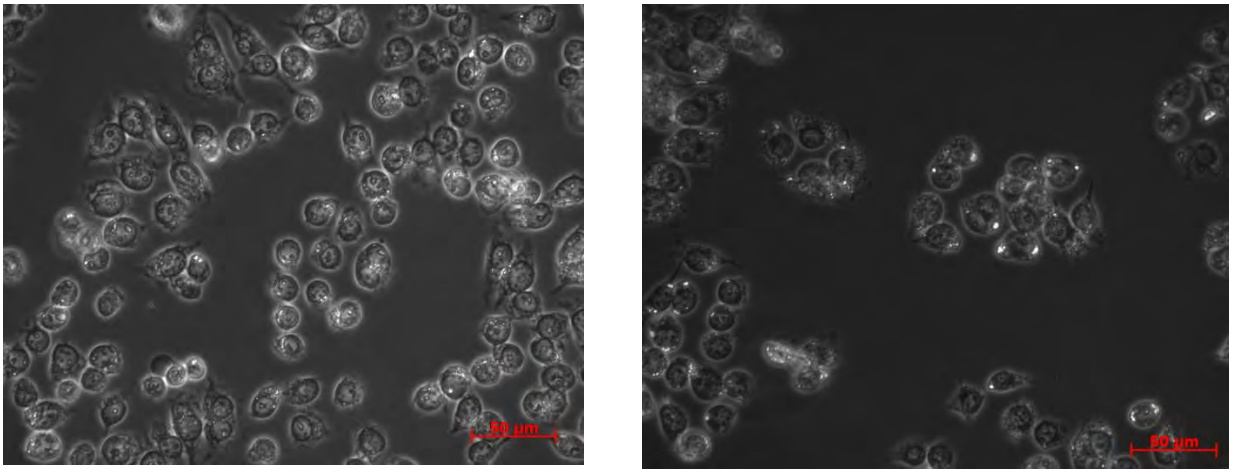

Figure 12: Phase contrast images of unpigmented A375 melanoma cells; 24 hours post-hypericin induced photodynamic therapy (HYP+L) (A) and combination induced photodynamic therapy (DTIC+HYP+L) treatment (B). A375 cells were cultured and sequentially exposed to 1250µM DTIC and 3µM HYP, for 24 hour. Images were captured 24 hour post-treatment. Magnification: 400x; Scale bar = 50µM.:

From the fluorescent images, the control cells displayed an intact round Hoechst positively; stained nucleus, which could be seen within the untreated A375 cells (Figure 13A). However, after HYP+L and DTIC+HYP+L treatments, the nuclei appeared smaller with formation of nuclear aggregates within the nucleus (Figure 14A & 14B, arrows). Finally, cytoplasmic localisation of hypericin (intracellular red colour, HYP, Figure 14 & 15) could be seen as a specific perinuclear aggregation represented by red punctae (Fig 14 & 15, arrows) in all A375 HYP- treated cells.

(A) (B)

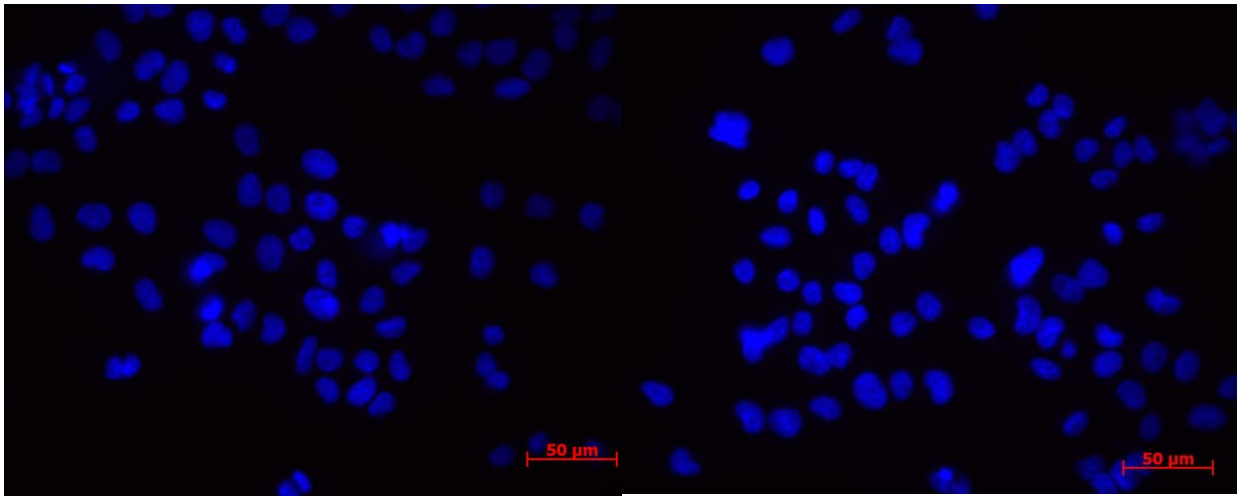

Figure 13: Fluorescent images of Hoechst stained nuclei (Blue) of unpigmented A375 melanoma cells (A) and dacarbazine A375 treated cells (B). A375 cells were cultured and exposed to 1250µM DTIC for 24 hour. Images of Hoechst stained A375 cells, were captured 24 hours post-treatment. Magnification: 400x; Scale bar = 50µM.

(A) (B)

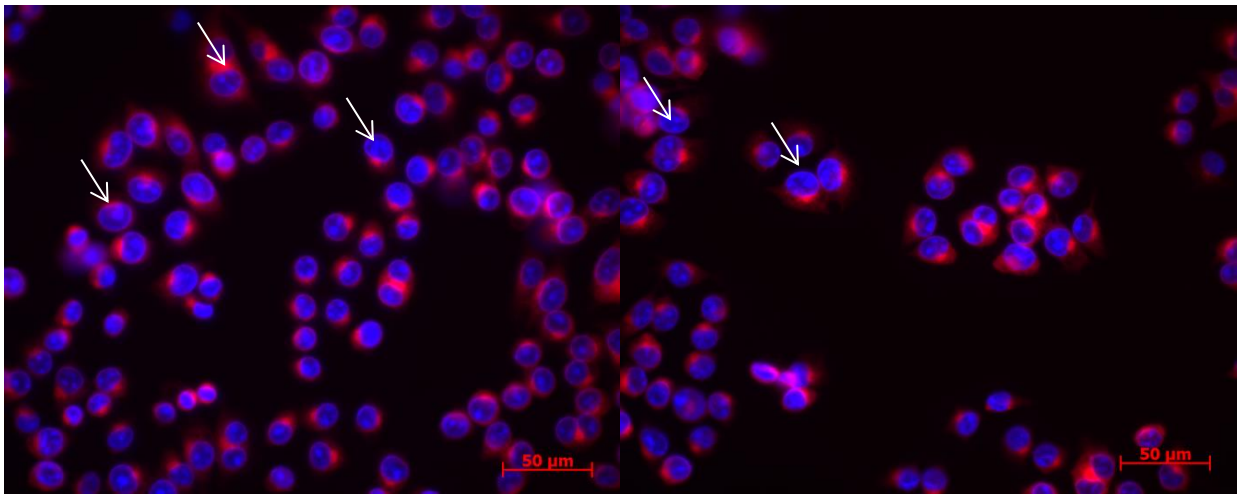

Figure 14: Fluorescent images of Hoechst stained nuclei (Blue) and hypericin (red) of unpigmented A375 melanoma cells; 24 hours post-hypericin induced photodynamic therapy (HYP+L) (A) and combination therapy treatment (DTIC+HYP+L) (B). A375 cells were cultured and sequentially exposed to 1250µM DTIC and 3µM HYP for 24 hour. Images of Hoechst and HYP stained A375 cells, were captured 24 hour post-treatment (arrow: nuclear aggregate). Magnification: 400x; Scale bar = 50µM.

(A) **(B)**

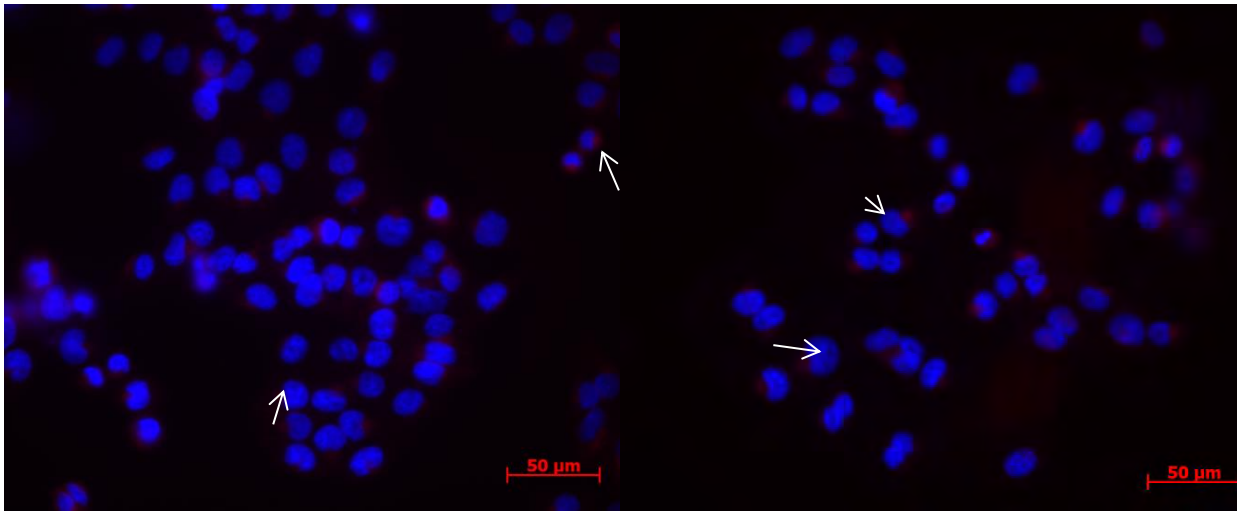

Figure 15: Fluorescent images of Hoechst stained nuclei (Blue) and hypericin (Red) of unpigmented melanoma cells treated with hypericin (HYP-L) (A) and combination treatment (DTIC+HYP-L). A375 cells were exposed sequentially to DTIC 1250µM and 3µM HYP for 24 hour. Images of Hoechst and HYP stained A375 cells, were captured 24 hour post-treatment (arrow: nuclear aggregate). Magnification: 400x; Scale bar = 50µM).

Control pigmented, UCT Mel1 cells exhibited a bipolar, dendritic morphology (Figure 16A). The DTIC and HYP-L treatments, resulted in an increased granularity and concomitant decreased dendricity (HYP treated group) when compared to their untreated controls (Figure 16 B & 17 A). Interestingly, DTIC+HYP-L treatment resulted in complete dendritic loss and flattening of the UCT-Mel1 cells (Figure 17B, arrow).

(A) **(B)**

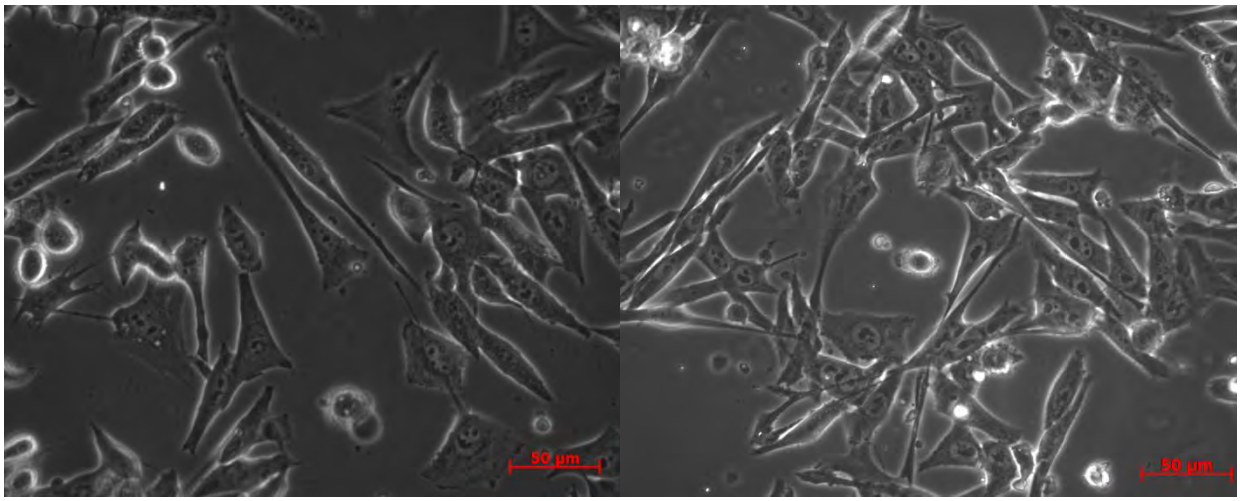

Figure 16: Phase contrast images of pigmented UCT-Mel1 melanoma cells (A) and dacarbazine treated UCT-Mel1 cells (B). UCT-Mel1 cells were cultured and exposed to 1250µM DTIC for 24 hours. Images were captured, 24 hour post-treatment. Magnification: 400x; Scale bar = 50µM.

(A) **(B)**

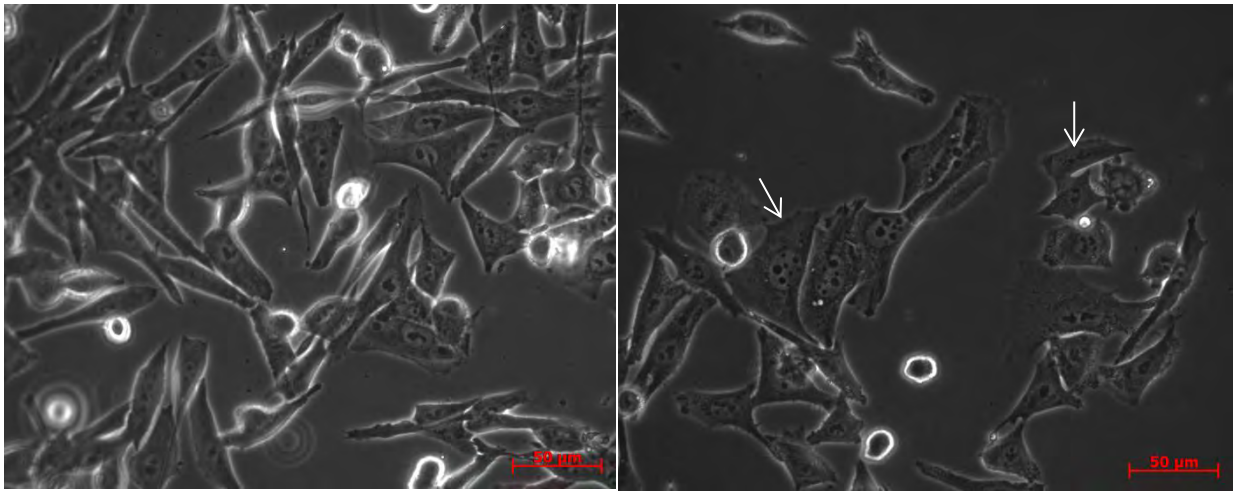

Figure 17: Phase contrast images of pigmented UCT-Mel1 melanoma cells; 24 hours post hypericin (HYP-L) (A) and combination therapy treatment (DTIC+HYP-L) (B). UCT-Mel1 cells were cultured and either exposed to 3µM HYP only or sequentially to 1250µM DTIC and HYP for 24hour. Images were captured 24 hour post-treatment (Loss of dendrites). Magnification: 400x; Scale bar = 50µM.

In addition, HYP+L and DTIC+HYP+L caused a drastic change in morphological features of UCT Mel1, with complete disruption of their cellular morphology with associated cytoplasmic shrinkage, cell flattening and multiple, narrow dendrites (Figure 18A & 18B, arrows).

(A) **(B)**

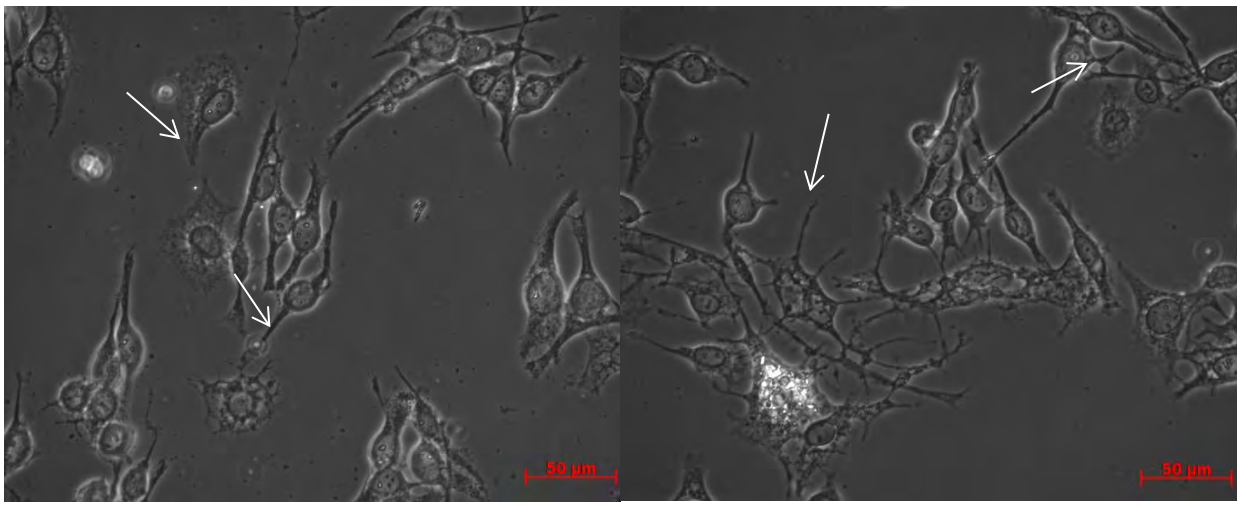

Figure 18: Phase contrast images of pigmented UCT-Mel1 melanoma cells; 24 hours post hypericin induced photodynamic therapy (HYP+L) (A) and combination therapy treatment (DTIC+HYP+L) (B). UCT-Mel1 cells were cultured and either exposed to HYP+L or sequentially to 1250µM DTIC and 3µM HYP (DTIC+HYP+L) for 24 hour. Images were captured 24 hour post-treatment (arrow: damaged and multi-dendritic cells). Magnification: 400x; Scale bar = 50µM.

In contrast, fluorescent images, displayed a conservation of nuclear integrity after all treatments (Figure 19, 20 and 21). Finally, a cytoplasmic and perinuclear localization of HYP (red colour in Figure 20 and 21) occurred around the nucleus in contrast to the red punctate pattern of localization in the A375s (Figure 20 & 21). From these observations, difference in cell morphology between pigmented (UCT-Mel1) and unpigmented melanoma (A375) could be seen, following HYP+L and DTIC+HYP+L particularly (Figure 12 & 18). This was of particular interest, as difference in nuclear integrity could be reflective of the sensitivity (or mode of cell death) of the different melanoma cell lines to the respective therapies observed in Figure 6, 7, 8 and 9.

(A) **(B)**

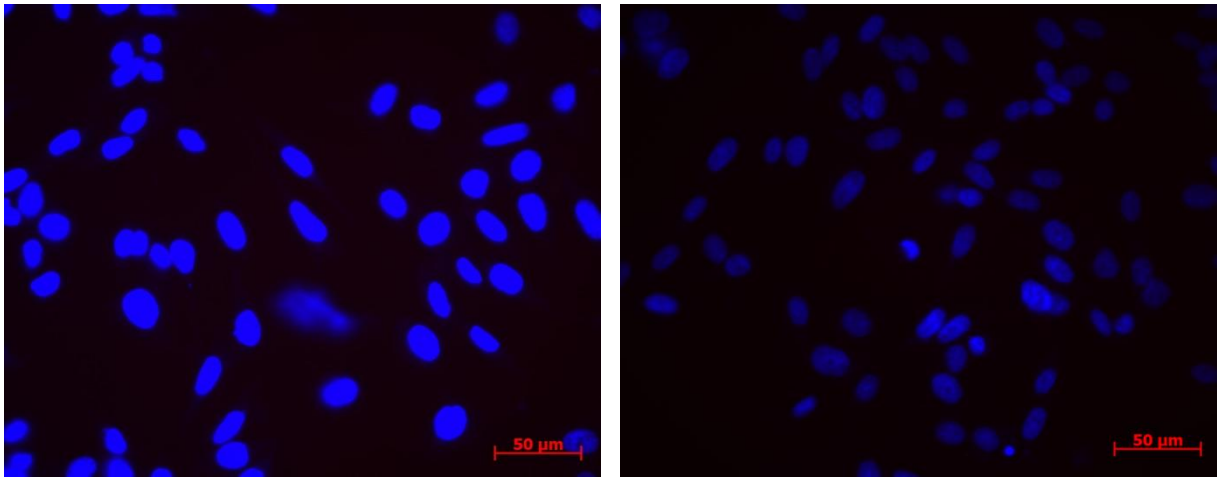

Figure 19: Fluorescent images of Hoechst stained nuclei (Blue) of pigmented UCT-Mel1 melanoma cells (A) and dacarbazine treated UCT-Mel1 cells (B). UCT-Mel1 cells were cultured and exposed to 1250µM DTIC for 24 hour. Images of Hoechst stained UCT-Mel1 cells, were captured 24 hours post-treatment. Magnification: 400x; Scale bar = 50µM.

(A) **(B)**

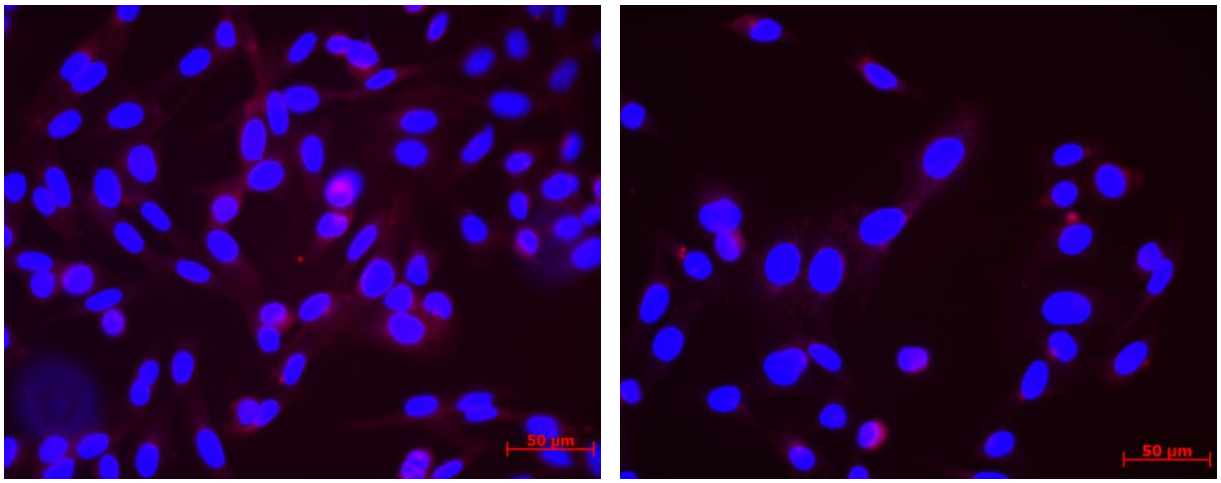

Figure 20: Fluorescent images of Hoechst stained (Blue) and hypericin (Red); 24 hour post-Hypericin (HYP-L) (A) and combination therapy (DTIC+HYP-L). UCT-Mel1 cells were cultured and either exposed to 3µM HYP only or sequentially to 1250µM DTIC and HYP for 24hour. Images were captured 24 hour post-treatment. Images of Hoechst and HYP stained UCT-Mel1 cells, were captured 24 hour post-treatment. Magnification: 400x; Scale bar= 50µM.

(A) (B)

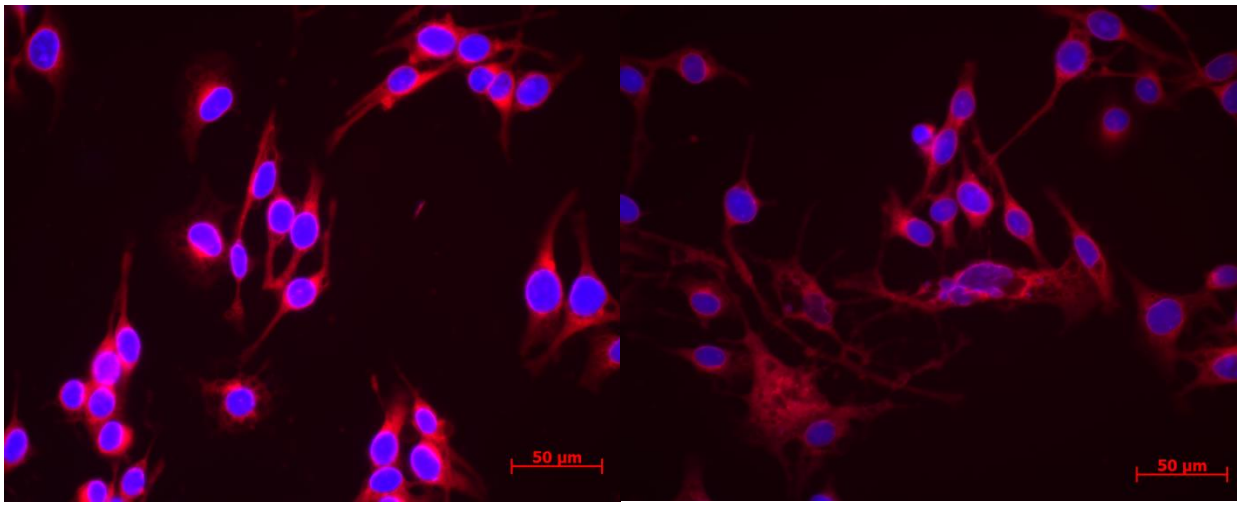

Figure 21: Fluorescent images of Hoechst stained nuclei (Blue) and hypericin (red) of pigmented UCT-Mel1 melanoma cells; 24 hours post-hypericin induced photodynamic therapy (HYP+L) (A) and combination therapy treatment (DTIC+HYP+L) B). UCT-Mel1 cells were cultured and sequentially exposed to 1250µM DTIC and 3µM HYP for 24 hour. Images of Hoechst and HYP stained UCT-Mel1 cells, were captured 24 hour post-treatment. Magnification: 400x; Scale bar = 50µM.

3.4. ASSESSMENT OF METASTATIC MELANOMA CLONOGENIC ACTIVITY 24HOURS POST-THERAPEUTIC TREATMENTS

As clonogenicity is a marker of tumorigenicity, the next objective was to determine the clonogenic capacity of the pigmented (UCT-Mel1) and unpigmented (A375) metastatic melanoma, 24 hours post-therapeutic treatments. As shown in Figure 22, 24h DTIC treatment was successful at significantly reducing the clonogenic activity of the A375 (unpigmented) melanoma cell lines, when compared to their control (Figure 22A). In contrast, the pigmented melanoma cells (UCT-Mel1) maintained their clonogenic activity despite DTIC treatment, (Figure 22B). Although upon DTIC treatment UCT-Mel1 cells were more clonogenic than the A375, they formed five times less colonies as compared to the A375 cells upon 7 days treatment (Figure 22). These observations clearly, re-enforced the resistance of UCT-Mel1 to the DTIC treatment (when compared to the A375), which nicely correlate with the cell viability, following DTIC treatment in Figure 6 & 7. Upon establishment of the two

metastatic melanoma cell lines clonogenic activity upon DTIC treatment, the next aim was to evaluate, the capacity of the combination therapy to better supress the clonogenic activity.

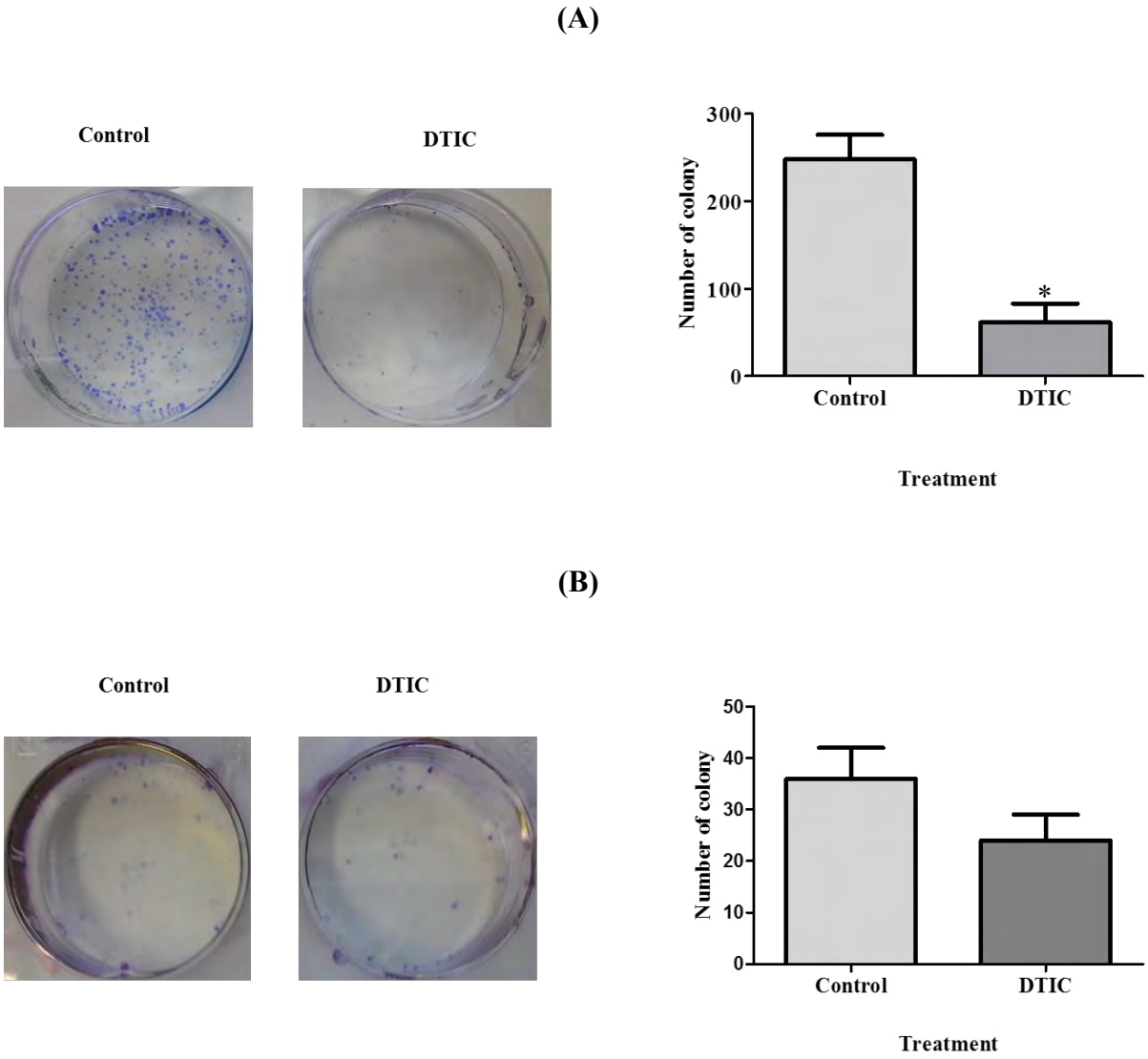

Figure 22: Clonogenic activity of pigmented (UCT-Mel1) and unpigmented melanoma (A375), 24 hours post DTIC treatment. A375 (A) and UCT-Mel1 melanoma cells (B) were exposed to 1250µM DTIC for 24 hours and re-plated post treatment at a lower density for clonogenic capacity assessment. Results are presented as numbers of colonies. (Significant difference = P *< 0.05. Statistical analysis T-test; n=2).

To assess the efficacy of the combination treatment, the clonogenic activities were analyzed after 24hours DTIC+HYP+L. Figures 23 and 24 show that both HYP+L and DTIC+HYP+L resulted in complete abrogation of the clonogenic activity in UCT-Mel1 and A375 melanoma cell lines, 24 hours post-treatment compared to their respective controls. Interestingly, the UCT-Mel1 displayed a 46.25% reduction in colony number compared to the 53% reduction in the A375 cells, following DTIC+HYP-L treatment, clearly illustrating the increased resistance/tumorigenicity of the pigmented melanomas (Figure 23 & 24). Due to the differential clonogenic activity observed, in response to the different therapeutic treatments on UCT-Mel1 and A375 melanoma cells, our next objective set to investigate the possible underlying resistance mechanism, causing therapeutic treatment failure.

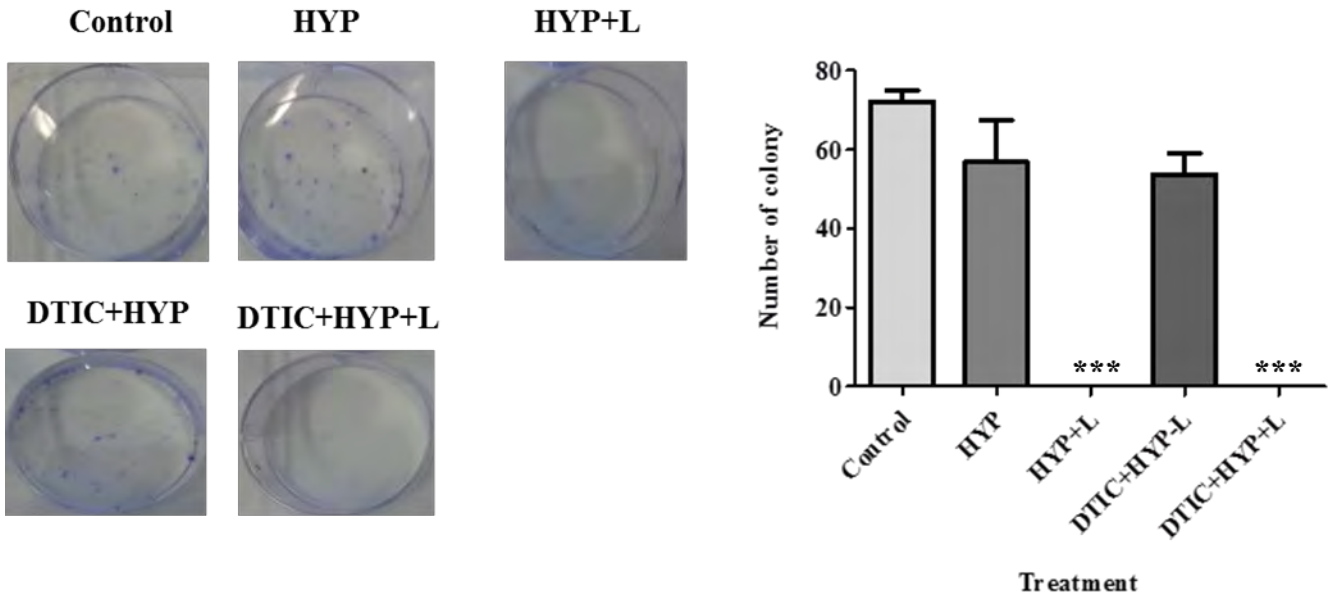

Figure 23: Clonogenic activity of pigmented metastatic melanoma (UCT-Mel1), 24 hours post combination therapy (DTIC+HYP-PDT) treatment. UCT-Mel1melanoma cells were sequentially exposed to DTIC and HYP-PDT for 24 hours. 24 hours post-treatment completion, UCT-Mel1 cells were re-plated at a lower density for clonogenic capacity assessment. Results were presented as numbers of colonies. (Significant difference = P *< 0.05. Statistical analysis T-test; n=2).

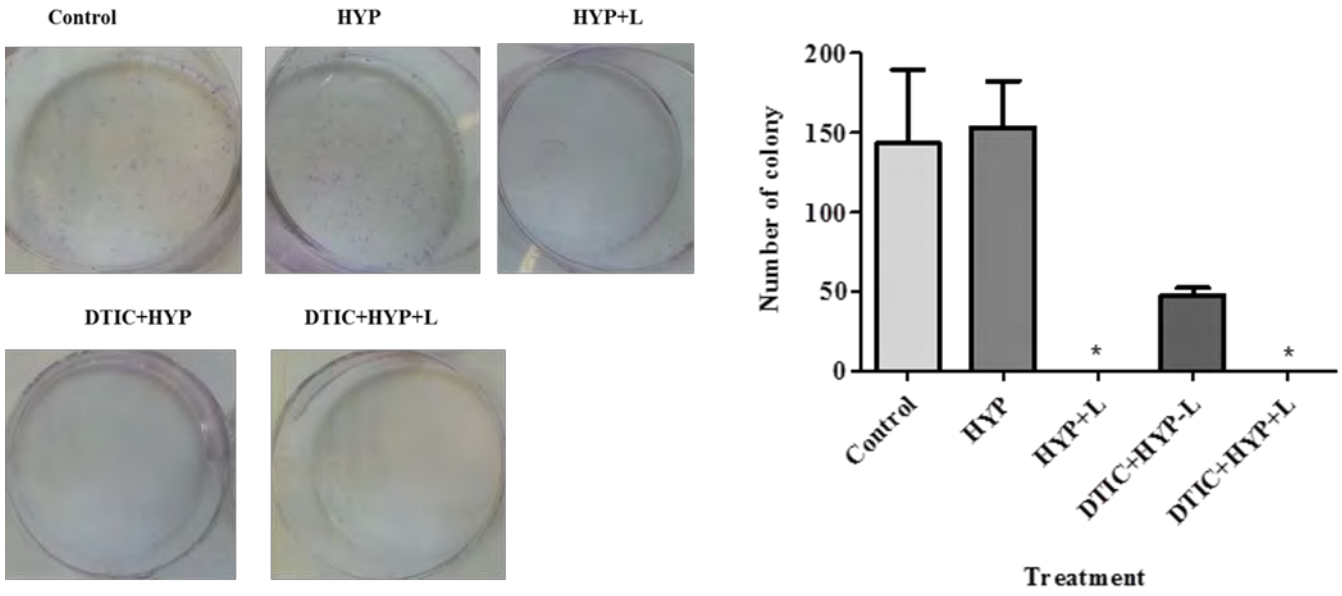

Figure 24: Clonogenic activity of unpigmented metastatic melanoma (A375), 24 hours post combination therapy (DTIC+HYP-PDT) treatment. A375 melanoma cells were sequentially exposed to 1250μM DTIC and HYP-PDT for 24hours. 24 hours post-treatment completion, A375 cells were re-plated at a lower density for clonogenic capacity assessment. Results were presented as numbers of colonies. (Significant difference = P *< 0.05. Statistical analysis T-test; n=2).

3.5. ABC TRANSPORTER PROTEIN EXPRESSION FOLLOWING THERAPEUTIC TREATMENTS

It is well documented that ABC transporters are involved in therapeutic treatment failure by lowering the accumulation of therapeutic drugs within cancer cells[13,22,93,106]. With this in mind, the next set of experiments aimed to establish ABC transporter protein expression before and after therapeutic treatments, to establish their possible contribution to therapy resistance in the melanoma cells.

Figures 25 and 26 clearly revealed that ABCG2 transporter expression was increased upon DTIC treatment (24hours) in both the A375 and UCT-Mel1 cells compared to their untreated controls. Interestingly, none of these increased expressions (ABCG2) showed significance (Figures 25 and 26).

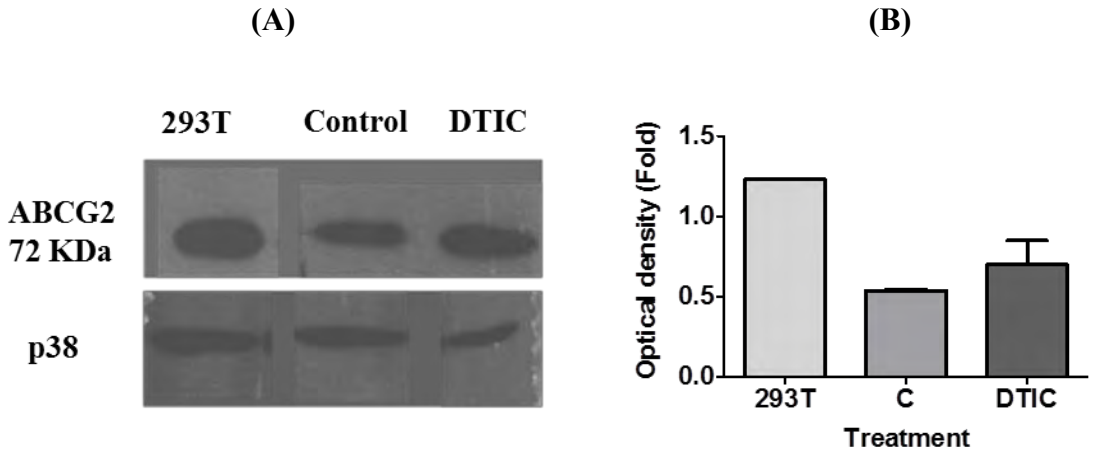

Figure 25: ABCG2 protein expression in unpigmented metastatic melanoma cells (A375), 24 hours post Dacarbazine (DTIC) treatment: Western blot of ABCG2 protein expression in 293T cells (positive control, human embryonic kidney cells), C (untreated control) and dacarbazine (DTIC) treatment (24 hours) **(A)**. Densitometry analysis showing the optical density (fold) of ABCG2 transporters, 24 hours post DTIC treatment. Data was normalized to the control, by obtaining the ratio of ABCG2 expression (band optical density) and its loading control, p38 **(B)**. No statistical significance was obtained using the student t-test ($^{*}P<0.05$) (n=3).

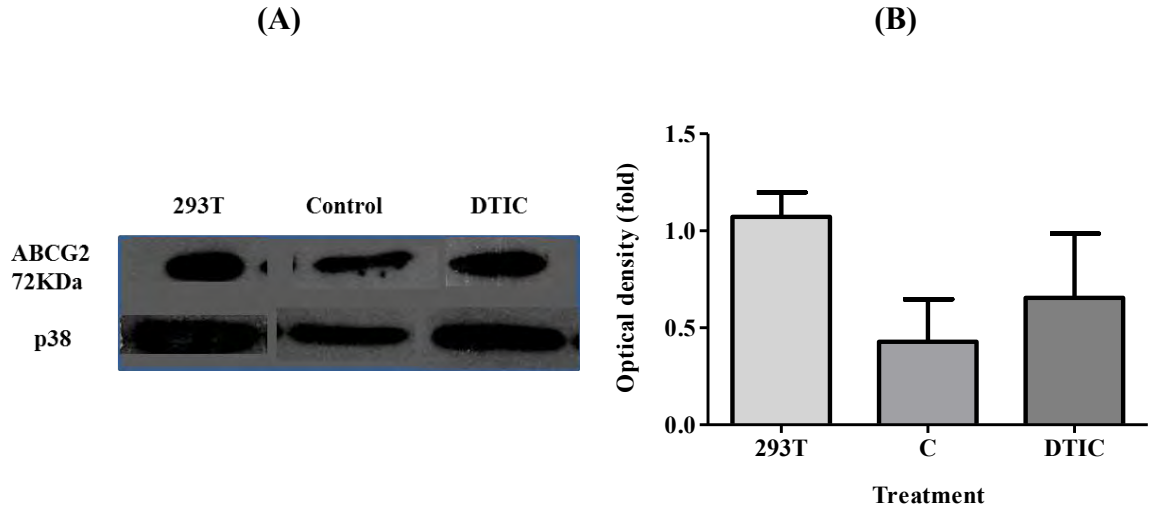

Figure 26: ABCG2 protein expression in pigmented metastatic melanoma cells (UCT-Mel1), 24 hours post Dacarbazine (DTIC) treatment: Western blot of ABCG2 protein expression in 293T

cells (positive control, human embryonic kidney cells), C (untreated control) and dacarbazine (DTIC) treatment (24 hours) **(A)**. Densitometry analysis, showing the optical density (fold) of ABCG2 transporters, 24 hours post DTIC treatment. Data was normalized to the control, by obtaining the ratio of ABCG2 expression (band optical density) and its loading control, p38 **(B)**. No statistical significance was obtained using the student t-test ($^{*}P<0.05$) (n=2).

Assessment of ABCB1 (also called multidrug resistance protein (MDR)) protein expression displayed an increase upon 24h DTIC treatment in UCT-Mel1 (during optimization where all the melanoma cells were collected), when compared to the control (Figure 27A). However, it should be noted that these cells represented all the cells and was not restricted to a resistant population. However, this was not reproducible upon additional experimental repeats in UCT-Mel1, as well as A375 melanoma cell lines (Figure 27B & 28). In future further experiments should involve harvesting of the total treated cell population (adherent and floating treated cells).

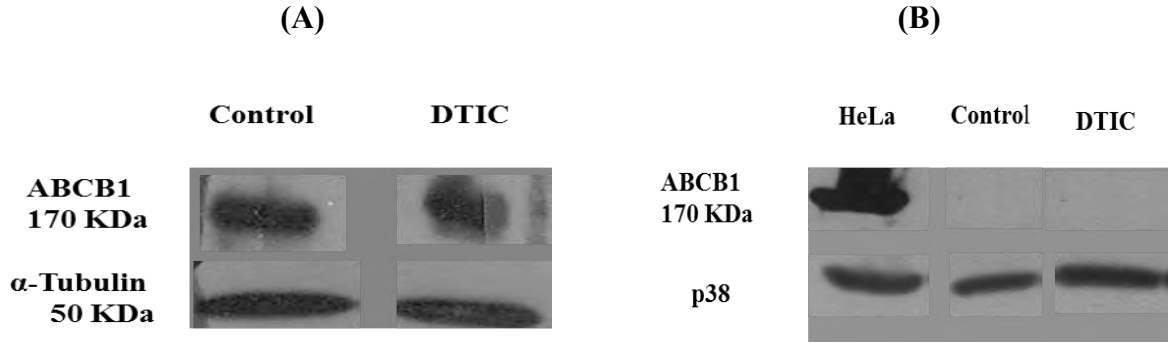

Figure 27: ABCB1 (MDR1) protein expression in pigmented metastatic melanoma cells (UCT-Mel1), 24 hours post Dacarbazine (DTIC) treatment: Western blot of ABCB1 protein expression in HeLa cells (positive control, human cervical cancer cells), C (untreated control) and dacarbazine (DTIC) treatment (24 hours) during optimization **(A)** and experimental repeat **(B)**. Results of ABCB1 expression were normalised to their respective loading control p38 (38KDa) (A) and α-Tubulin (50KDa).

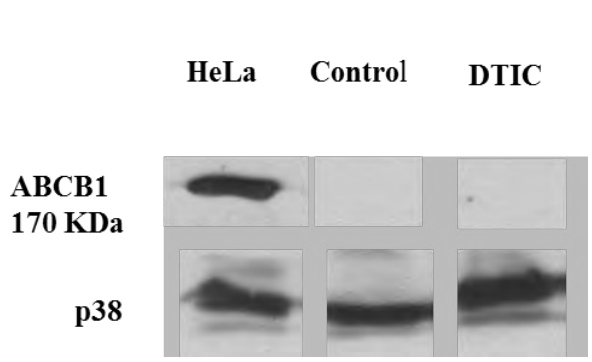

Figure 28: ABCB1 (MDR1) protein expression in unpigmented metastatic melanoma cells (A375), 24 hours post Dacarbazine (DTIC) treatment: Western blot of ABCB1 protein expression in HeLa cells (positive control, human liver cancer cells), C (untreated control) and dacarbazine (DTIC) treatment (24 hours). Results of ABCB1 expression was normalised to the loading control p38 (38KDa).

Moreover, detection of the ABCB5 expression, which is specifically overexpressed in melanoma upon chemotherapy treatment[13], was observed upon DTIC treatment and control cells (Figure 29). Finally, no ABCG2 expression was detected in the two melanoma cell lines upon exposure to combination therapy (Figure 30).

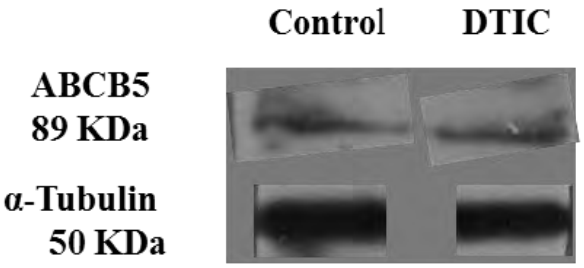

Figure 29: ABCB5 protein expression in pigmented metastatic melanoma cells (UCT-Mel1), 24 hours post Dacarbazine (DTIC) treatment: Western blot of optimized ABCB5 protein expression in pigmented melanoma cells, C (untreated control) and dacarbazine (DTIC) treatment (24 hours) (A). Results of ABCB5 expression were normalised to their respective loading control α-Tubulin (50KDa)

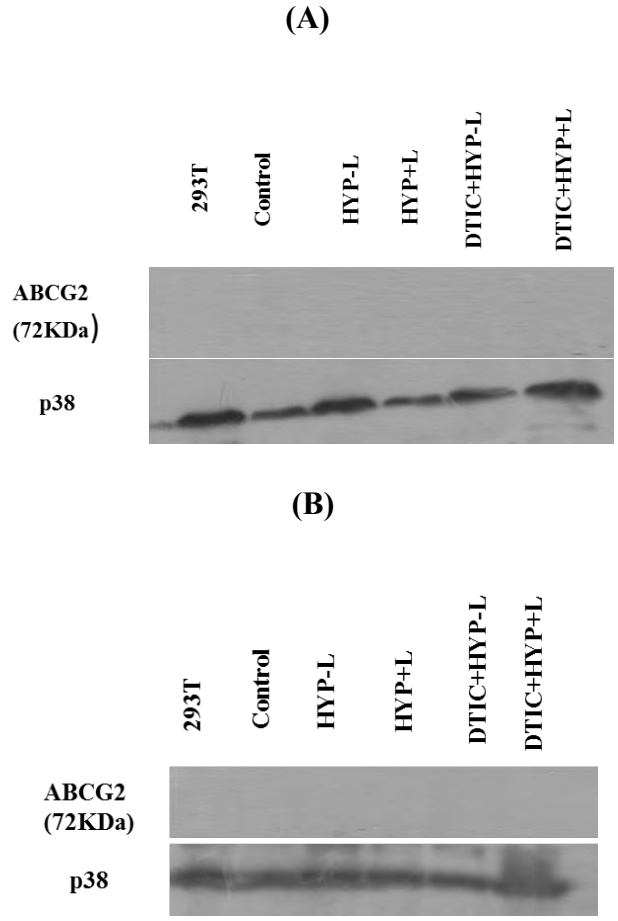

Figure 30: ABCG2 protein expression in pigmented (UCT-Mel1) and unpigmented (A375) metastatic melanoma cells (UCT-Mel1), 24 hours post-combination therapy treatment: Western blot of ABCG2 protein expression in 293T cells (positive control, human embryonic kidney cells), C (untreated control) and dacarbazine (DTIC) treatment (24 hours) in UCT-Mel1 **(A)** and A375 **(B)**. Data was normalized to the control, by obtaining the ratio of ABCG2 expression (band optical density) and its loading control, p38 (38 KDa).

Chapter 4: Discussion

Despite extensive research and clinical trials, the prognosis and survival of metastatic melanoma remains dismal. Early detection of localized melanoma may be cured through surgery however there is no therapy for metastatic melanoma or melanoma with metastatic potential. In addition, recurrence rates of resected melanoma remain high. Because melanoma is inherently resistant to traditional forms of chemotherapy and radiotherapy 1, various strategies have been developed for treatments which include immunotherapy eg. Interleukin-2 (IL-2) 2, radiotherapy 3 biochemotherapy 4-7 and gene therapy 2, 8, the application of newer therapies are pertinent. Photodynamic therapy (PDT) is one such therapy. More recently, cocktails and combination therapies have been introduced in an attempt to not only eradicate the melanoma tumorigenic cells abut also reduce the resistance of the remaining cancer cells. With this in mind, the central aim of this project was, through combination of chemotherapy (DTIC) and HYP-PDT, to investigate their possible synergistic action in melanoma skin cancer. This was rendered possible by firstly determining the lethal dose of DTIC killing 50% of the melanoma cells (UCT-Mel1 and A375). Treatment (24 hour) of the pigmented (UCT-Mel1) (Figure 6A) and unpigmented (A375) melanoma cells, with increasing DTIC concentrations (0.48-3 mM) displayed cytotoxicity towards the A375 cells only (Figure 6B). However, when the treatment was prolonged for an additional 24 hours (48hour treatment in total), a reduction in cell viability of the pigmented UCT-Mel1 cells (22.3%) could be observed at1.5mM DTIC treatment (Figure 7A). The equivalent dose at this time point in the A375 cells led to a 54.64% cell viability (Figure 7B). These results suggest that pigmented melanoma (UCT-Mel1) is more resistant to chemotherapeutic treatment (DTIC), compared to unpigmented melanoma. This observed resistance in the pigmented cells is not that unexpected as both our earlier work[27,47] attribute resistance in pigmented cells to the presence of melanin acting as an antioxidant to neutralize ROS and melanosomes acting as a "sink" to "mop up" chemotherapeutic drugs, leading to treatment failure. Interestingly though, in this scenario, it seems that the presence of melanin is the greater resistant mechanism as A375 cells have functional melanosomes present in their cytoplasm, they are just devoid of melanin.

As previous work in our lab had determined 3μM Hypericin (3μM HYP) to be lethal to UCT-Mel1 and A375 melanoma cells 24 hour post-treatment [46], this concentration was used in combination with our DTIC lethal dose (1250μM) to investigate cell resistance

Twenty four hour treatment analyses of the UCT-Mel1 cell viability (Figure 8A) revealed that the DTIC exposed to light (DTIC+L) was not lethal to the cells (3.6% reduction). However, when the cells were treated with activated hypericin (HYP+L) or the combination treatment (DTIC+HYP+L) a significant reduction in cell viability was obtained (50.19% & 61.26%, respectively). This lethal effect (DTIC+HYP+L, Figure 8B), was further pronounced upon 48 hour treatment of the UCT-Mel1 cells with a resultant reduction of 77.75% in cell viability. However, this was not a result of synergism between the HYP+L and DTIC+HYP+L, as no significant difference was obtained between the two. In comparison to the UCT-Mel1 cells, treatment of A375 cells at both time points (24 & 48 hour) resulted in a better therapeutic outcome, respectively causing 25% (DTIC+L), 55.1% (HYP+L) and 65.7% (DTIC+HYP+L) reduction in cell viability at 24 hour (Figure 9A) and a further 50, 66 and 83.2% cell viabilities at 48 hour after treatment (Figure 9B). Taken together these results showed that UCT-Mel1 were still more resistant to the therapeutic treatment, when compared to the A375 cells. Previous results in our laboratory strengthen the postulate that pigmentation may play a role in resistance of these melanoma cells to PDT. However, to be sure of this theory, future work directed at the chemosensitivity will have to involve experiments in an identical cell line that is more or less pigmented. Interestingly, corroborating recent work showed not only that hypericin localized in melanosomes, but also but that the melanosomes were involved in the eradication of drugs entering melanocytic cells[47,42,60].

Once the cytotoxic profile of the chemotherapeutic (DTIC) and combination therapy treatments were acquired, the next objective was to analyses the morphological changes associated with the cellular response to these treatments. Morphologically, the HYP+L and DTIC+HYP+L treatments revealed complete disruption in cellular morphology associated with increased vacuolization in A375 and cytoplasmic shrinkage in UCT-Mel1 melanoma cells. In addition, cell shrinkage was observed in both cell lines, this with increased in granularity and cell swelling in A375, as opposed to the UCT-Mel1, where cells with multiple morphology (Flattened, multiple narrow dendrites) were depicted (Figure 12 and 18). These cell dependent morphological changes were further amplified through the fluorescent images, displaying different HYP distribution and nuclear integrity resulting from the treatments in both cell lines (Figure 14 and 21). This was characterized by specific punctate, perinuclear aggregation of the HYP in A375, as opposed to a homogenous distribution of HYP around the nucleus in UCT-Mel1 (Figure 14 and 21). Although

cytoplasmic localization of HYP was observed in both cell lines, difference in nuclear integrity was detected. In the A375 cells, formation of small nuclear aggregates was observed, when compared to the UCT-Mel1 where nuclear integrity was conserved (Figure 14 and 21). These morphological differences in the two melanoma cell lines, could suggest different modes of cell death. According to Davids et al. (2008) and Kleeman et al. (2014), HYP-PDT induces a necrotic mode of cell death in the UCT-Mel1, while activating an apoptotic mode of cell death in A375 cells[46,42]. Similarly, the increased vacuolization observed in A375 could be indicating an apoptotic mode of cell death. However, increased vacuolization could also be evidence of autophagy and a resultant attempt of the cells to resist the treatment. It is more plausible that these cells are dying by apoptosis as Kleeman et al. (2014), showed HYP to co-localize in lysosomes, endoplasmic reticulum (ER), mitochondria and melanosomes of these cells with a resultant extrinsic (A375 cells) and intrinsic (UCT-Mel1) caspase-dependent mode of cell death[42]. Further analyses would be needed to delineate these differences. The complete morphological disruption depicted in UCT-Mel1 upon treatments (HYP+L and DTIC+HYP+L) is clear evidence of necrosis.

Clonogenic analyses are reflective of the tumorigenicity of cancer cells. The premise is that the more clonal the cells, the more likely they are to form tumors. Our analyses revealed that exposure of the two melanoma cell lines to hypericin (HYP-L), DTIC only and the combination without light activation (DTIC+HYP-L) showed that the A375 cells were more sensitive i.e. created less colonies compared to the UCT-Mel1 (Figure 22, 23 and 24). The resistance observed in UCT-Mel1, upon DTIC and DTIC+HYP-L treatment correlated with its cell viability results (Figure 6, 7, 8 and 9) and could possibly be related to the development of a side population having stem cells properties[111]. These side stem cell like population cells are therapeutically resistant cells (different from the main resistant population), slow cycling cells, found to overexpress specific ABC transporter proteins (ABCB5 and ABCB1), grow under hypoxic conditions and re-form the parental tumor causing the clinically observed relapse [10,82, 93, 119, 120, 110]. In contrast, exposure of the two melanoma cell lines to treatment (HYP+L and DTIC+HYP+L) resulted in complete abrogation of their clonogenic activities (Figure 23 and 24). This would imply that the treatment, with HYP+L only or in combination completely destroys the side population cells, making it a potentially effective treatment option.

As this side population confers resistance, and the fact that this resistance may be due to increased ABC transporter expression, our next objective was to determine the ABC transporter (ABCB1, ABCB5 and ABCG2) protein expression before and after DTIC and combination therapy treatment.

In cancer, ABC transporters have been implicated in resistance to therapeutic treatments, by lowering the intracellular accumulation of cytotoxic drugs, below their cytotoxic threshold[3, 22,193]. Although the expression of these transporters are said to be specific in response to the exposure of certain cytotoxic drugs, the overall expression is varied with respect to types of treatments and cancers treated. These transporter expressions are often related to functional requirements of the cell. For example, ABCG2, also known as the breast cancer resistant protein (BCRP) has been involved in resistance to cytotoxic drugs [105,106, 121]. For this reason, we concentrated on the expression levels of ABCB1/MDR, ABCB5 and ABCG2/BCRP. Our results showed that ABCG2 expression was increased after 24 hour DTIC treatment only in both the A375 and UCT-Mel1 cells. The expression in the A375 cells corroborated recent work of Wu et al. (2013), who showed that overexpression of ABCG2 in A375 melanoma cells, resulted in vemurafenib chemotherapeutic treatment failure[102]. Furthermore in the same cell type (A375), Goler-Baron et al. (2012) showed that photodestruction of ABCG2 rich extracellular vesicles (sequestering chemotherapeutic drugs, imidazoacridinones and topotecan) sensitized the cells to therapeutic treatment. To our knowledge, no reports thus far have highlighted the increase in expression of the ABCG2 transporters in pigmented melanoma cells. It is clear from our results and the literature that increased ABCG2 expression is a direct result of cell exposure to chemotherapeutic drugs. The results of this study however, further emphasize that this increased expression is chemo-specific and that the presence of melanin (UCT-Mel1) has no effect in increasing resistance and/or decreasing the expression of ABCG2.

Having established the expression of ABCG2 in both UCT-Mel1 and A375 cells upon DTIC treatment (24hour), we next attempted to determine its expression using the combination therapy (DTIC+HYP-L, DTIC+HYP+L, HYP-L and HYP+L). Our results showed that upon combination therapy treatment, no detection of ABCG2 protein expression in either the UCT-Mel1 or A375 cells. Unfortunately, this seemed to be related to the quality of the antibody, as no expression could be detected in the positive control 293T cells. Numerous attempts at optimizing further antibody concentrations and conditions resulted in no better results.

The ABCB1 transporter expression is related to multi-drug resistance protein (MDR), which is involved in resistance to chemotherapy[93,122,123]. Analysis of the ABCB1 transporter expression in our system initially revealed an increased expression upon 24 hour DTIC treatment (see Figure 27A). However, despite numerous repeated attempts, no detection of the transporter (ABCB1) could be obtained in either the UCT-Mel1or A375 cells (Figure 27B and 28). Two plausible reasons for this could be related to the percentage of the resistant population and ii) that only adherent cells were harvested for ABCB1 protein detection. According to the literature, the melanoma resistant populations overexpressing the ABC transporters (ABCB1, 5 and ABCG2) represent between 0.1 to 5% of the total tumor populations[110,124,94]. Knowing that only the adherent cells were harvested for ABC transporters protein expression, this could have resulted in a dilution of the melanoma cells fraction overexpressing these proteins. The possibility of it being due to an antibody detection issue was ruled out as detection of this transporter in positive control (Hela cells) cells displayed positivity (Figure 27B & 28). In future, further experiments should involve harvesting of the total treated cell population (adherent and floating cells). Despite the fact that this experiment was not reproducible, the increased detection level upon DTIC treatment would suggest that UCT-Mel1 may partly develop resistance to DTIC, by overexpressing the ABCB1, as has been reported in A375 melanoma cells and other cancers [93,94].

Finally, we analyzed ABCB5 expression, which is involved in melanoma resistance to DTIC chemotherapy[13]. Our results of both pre and post DTIC treatment showed that both control and DTIC treated UCT-Mel1 cells expressed ABCB5 (Figure 29). However, as in the case of the ABCB1 transporter results, no definitive expression levels could be detected which we suspect could be due to the fact that only the adherent cell population was harvested. A limitation to this result was certainly the lack of a positive control i.e. cells overexpressing ABCB5. A future attempt to confirm the expression of ABCB5 could involve transfection of any cell line with a plasmid containing the ABCB5 gene. Thus, to our knowledge, no positive control for ABCB5 exists currently. However assessment of the ABCB1 and ABCB5 expression were not performed, due to the detection problems encountered upon chemotherapy treatment.

Overall, these results demonstrated that melanoma resistance to chemo and combination phototherapies are dependent on the pigmented phenotype and possibly their expression of the ABC transporters within the cells. This was reflected by the UCT Mel1 resistant to

chemotherapy and combination therapy when compared to their unpigmented counterpart. This correlated with the clonogenic activity upon chemotherapeutic treatment. Interestingly, the combination therapy concomitantly abrogated the resistant phenotypes in both cell lines. This observation matched the morphological differences obtained after treatment in both cell types. Furthermore, these observed resistance features were shown to correlate with increased ABCG2 protein expression. However, expressions of ABCB1 and ABCB5 in response to DTIC treatment were inconclusive.

4.1. FUTURE RESEARCH

Although a number of novel conclusions have been drawn from this work, to strengthen the research even further, several points could be included. These are:

- Further experiments should involve harvesting of the total treated cell population (adherent and floating cells);
- A future attempt to confirm the expression of ABCB5 could involve transfection of any cell line with a plasmid containing the ABCB5 gene. This would be invaluable to future cancer research and further exploration of resistance mechanisms;
- Determination of the resistant population over-expressing the ABC transporters (ABCG2, ABCB1 and ABCB5) using fluorescent-activated cell sorting (FACS);
- Once this is determined, characterization of this population could be done to detect "stemness" markers;
- This population could then be expanded and further characterized over a timeframe to determine resistance markers within the clonal sub-population and parental populations.

REFERENCES:

1. Madan V, Lear JT, Szeimies R-M. Non-melanoma skin cancer. *Lancet*. 2010;375(9715):673-685. doi:10.1016/S0140-6736(09)61196-X.

2. Carlson JA, Ross JS, Slominski AJ. New techniques in dermatopathology that help to diagnose and prognosticate melanoma. *Clin Dermatol*. 2009;27(1):75-102. doi:10.1016/j.clindermatol.2008.09.007.

3. Ortonne J. Photoprotective properties of skin melanin. *Br J Dermatol*. 2002;146:7-10.

4. Stanojeviæ M, Stanojeviæ Z, Jovanoviæ D, Stojiljkoviæ M. Ultraviolet radiation and melanogenesis. *Arch Oncol*. 2004;12(4):203-205.

5. Huang Y, Vecchio D, Avci P, Yin R, Garcia-diaz M, Hamblin MR. Melanoma resistance to photodynamic therapy : new insights. *Biol Chem*. 2014;394(2):239-250. doi:10.1515/hsz-2012-0228.Melanoma.

6. Boyle P. Cancer of the skin: a forgotten problem in Europe. *Ann Oncol*. 2004;15(1):5-6. doi:10.1093/annonc/mdh032.

7. Miller AJ, Mihm MC. Mechanisms of disease Melanoma. *New Engl J Med*. 2006;355:51-65.

8. Pawlik TM, Sondak VK. Malignant melanoma: current state of primary and adjuvant treatment. *Crit Rev Oncol Hematol*. 2003;45(3):245-264.

9. Elliott AM, Al-Hajj M a. ABCB8 mediates doxorubicin resistance in melanoma cells by protecting the mitochondrial genome. *Mol Cancer Res*. 2009;7(1):79-87. doi:10.1158/1541-7786.MCR-08-0235.

10. Frank NY, Pendse SS, Lapchak PH, et al. Regulation of progenitor cell fusion by ABCB5 P-glycoprotein, a novel human ATP-binding cassette transporter. *J Biol Chem*. 2003;278(47):47156-47165. doi:10.1074/jbc.M308700200.

11. Siegel R, Naishadham D, Jemal A. Cancer statistics, 2012. *CA Cancer J Clin*. 62(1):10-29. doi:10.3322/caac.20138.

12. Jemal A, Siegel R, Ward E, et al. Cancer statistics, 2008. *CA Cancer J Clin*. 58(2):71-96. doi:10.3322/CA.2007.0010.

13. Chartrain M, Riond J, Stennevin A, et al. Melanoma chemotherapy leads to the selection of ABCB5-expressing cells. *PLoS One*. 2012;7(5):e36762. doi:10.1371/journal.pone.0036762.

14. Bhatia S, Tykodi SS, Thompson J a. Treatment of metastatic melanoma: an overview. *Oncology (Williston Park)*. 2009;23(6):488-496.

http://www.pubmedcentral.nih.gov/articlerender.fcgi?artid=2737459&tool=pmcentrez&rendertype=abstract.

15. Jablonski NG. *Skin: A Natural History*. California: University of California; 2006:266.

16. Augustine CK, Yoo JS, Potti A, et al. Genomic and molecular profiling predicts response to temozolomide in melanoma. *Clin Cancer Res*. 2009;15(2):502-510. doi:10.1158/1078-0432.CCR-08-1916.

17. Palathinkal DM1, Sharma TR, Koon HB BJ. Current systemic therapies for melanoma . *Dermatol Surg*. 2014;40(9):25072125. doi:10.1097/01.DSS.0000452626.09513.55.Current.

18. Ingram I. FDA Approves Anti-PD-1 Drug for Advanced Melanoma. *cancer Netw home J Oncol*. 2014:4-5.

19. Foletto MC, Haas SE. Cutaneous melanoma : new advances in treatment *. *An Bras Dermatol*. 2014;89(2):301-310.

20. Federici C, Petrucci F, Caimi S, et al. Exosome Release and Low pH Belong to a Framework of Resistance of Human Melanoma Cells to Cisplatin. *PLoS One*. 2014;9(2):e88193. doi:10.1371/journal.pone.0088193.

21. Tentori L, Lacal PM, Graziani G. Challenging resistance mechanisms to therapies for metastatic melanoma. *Trends Pharmacol Sci*. 2013;34(12):656-666. doi:10.1016/j.tips.2013.10.003.

22. Wu C, Sim H, Huang Y, Liu Y, Hsiao S. Overexpression of ATP-binding cassette transporter ABCG2 as a potential mechanism of acquired resistance to vemurafenib in BRAF (V600E) mutant cancer cells. *Biochem Pharmacol*. 2013;85(3):325-334. doi:10.1016/j.bcp.2012.11.003.

23. Spagnolo F, Queirolo P. Upcoming strategies for the treatment of metastatic melanoma. *Arch Dermatol Res*. 2012;304(3):177-184. doi:10.1007/s00403-012-1223-7.

24. Agostinis P, Berg K, Cengel KA, et al. Photodynamic Therapy of Cancer : An Update. *CA Cancer J Clin*. 2011;61:250-281. doi:10.3322/caac.20114.Available.

25. Gilaberte Y, Milla L, Salazar N, et al. Cellular Intrinsic Factors Involved in the Resistance of Squamous Cell Carcinoma to Photodynamic Therapy. *J Invest Dermatol*. 2014;134. doi:10.1038/jid.2014.178.

26. Davids LM, Kleemann B, Cooper S, Kidson SH. Melanomas display increased cytoprotection to hypericin-mediated cytotoxicity through the induction of autophagy. *Cell Biol Int*. 2009;33(10):1065-1072. doi:10.1016/j.cellbi.2009.06.026.

27. Sharma K V, Davids LM. Depigmentation in melanomas increases the efficacy of hypericin-mediated photodynamic-induced cell death. *Photodiagnosis Photodyn Ther*. 2011;9(2):156-163. doi:10.1016/j.pdpdt.2011.09.003.

28. Ahn J-C, Biswas R, Mondal A, Lee Y-K, Chung P-S. Cisplatin enhances the efficacy of 5-Aminolevulinic acid mediated photodynamic therapy in human head and neck squamous cell carcinoma. *Gen Physiol Biophys*. 2013;July 12 ep. doi:10.4149/gpb_2013046.

29. Sazgarnia A, Montazerabadi AR, Bahreyni-Toosi MH, Ahmadi A. Photosensitizing and radiosensitizing effects of mitoxantrone: combined chemo-, photo-, and radiotherapy of DFW human melanoma cells. *Lasers Med Sci*. 2013. doi:10.1007/s10103-013-1275-8.

30. Goler-Baron V, Assaraf YG. Overcoming multidrug resistance via photodestruction of ABCG2-rich extracellular vesicles sequestering photosensitive chemotherapeutics. *PLoS One*. 2012;7(4):e35487. doi:10.1371/journal.pone.0035487.

31. Sharma K V, Davids LM. Hypericin-PDT-induced rapid necrotic death in human squamous cell carcinoma cultures after multiple treatment. *Cell Biol Int*. 2012;36(12):1261-1266. doi:10.1042/CBI20120108.

32. Kawczyk-Krupka A, Bugaj AM, Latos W, Zaremba K, Sieroń A. Photodynamic therapy in treatment of cutaneous and choroidal melanoma. *Photodiagnosis Photodyn Ther*. 2013;10(4):503-509. doi:10.1016/j.pdpdt.2013.05.006.

33. Jendzelovský R, Mikes J, Koval' J, et al. Drug efflux transporters, MRP1 and BCRP, affect the outcome of hypericin-mediated photodynamic therapy in HT-29 adenocarcinoma cells. *Photochem Photobiol Sci*. 2009;8(12):1716-1723. doi:10.1039/b9pp00086k.

34. Baldea I, Filip AG, Napoca C-. Photodynamic therapy in melanoma an update. *J Physiol Pharmacol*. 2012;63(7):109-118.

35. Moan J, Berg K. Differential effects of glucose deprivation on the cellular sensitivity towards photodynamic treatment-based production of reactive oxygen species and apoptosis-induction. *Photochem Photobiol*. 1991;53(4):1991.

36. Uzdensky AB, Ma LW, Iani V, Hjortland GO, Steen HB, Moan J. Intracellular localisation of hypericin in human glioblastoma and carcinoma cell lines. *Lasers Med Sci*. 2001;16(4):276-283. http://www.ncbi.nlm.nih.gov/pubmed/11702633. Accessed September 27, 2013.

37. Ritz R, Roser F, Radomski N, Strauss WSL, Tatagiba M, Gharabaghi A. Subcellular colocalization of hypericin with respect to endoplasmic reticulum and Golgi apparatus in glioblastoma cells. *Anticancer Res*. 28(4B):2033-2038. http://www.ncbi.nlm.nih.gov/pubmed/18751371. Accessed September 27, 2013.

38. Robertson C a, Evans DH, Abrahamse H. Photodynamic therapy (PDT): a short review on cellular mechanisms and cancer research applications for PDT. *J Photochem Photobiol B*. 2009;96(1):1-8. doi:10.1016/j.jphotobiol.2009.04.001.

39. Maduray K, Odhav B, Nyokong T. In vitro photodynamic effect of aluminum tetrasulfophthalocyanines on melanoma skin cancer and healthy normal skin cells. *Photodiagnosis Photodyn Ther*. 2012;9(1):32-39. doi:10.1016/j.pdpdt.2011.07.001.

40. Maduray K, Karsten A, Odhav B, Nyokong T. In vitro toxicity testing of zinc tetrasulfophthalocyanines in fibroblast and keratinocyte cells for the treatment of melanoma cancer by photodynamic therapy. *J Photochem Photobiol B*. 2011;103(2):98-104. doi:10.1016/j.jphotobiol.2011.01.020.

41. Sheleg S V, Zhavrid EA, Khodina T V, et al. Photodynamic therapy with chlorin e(6) for skin metastases of melanoma. *Photodermatol Photoimmunol Photomed*. 2004;20(1):21-26. http://www.ncbi.nlm.nih.gov/pubmed/14738529. Accessed October 28, 2014.

42. Kleemann B, Loos B, Scriba TJ, Lang D, Davids LM. St John's Wort (Hypericum perforatum L.) photomedicine: hypericin-photodynamic therapy induces metastatic melanoma cell death. *PLoS One*. 2014;9(7):e103762. doi:10.1371/journal.pone.0103762.

43. Saczko J, Kulbacka J, Chwiłkowska a, et al. The influence of photodynamic therapy on apoptosis in human melanoma cell line. *Folia Histochem Cytobiol*. 2005;43(3):129-132. http://www.ncbi.nlm.nih.gov/pubmed/16201311.

44. Robertson CA, Abrahamse H, Evans D. The in vitro PDT efficacy of a novel metallophthalocyanine (MPc) derivative and established 5-ALA photosensitizing dyes against human metastatic melanoma cells. *Lasers Surg Med*. 2010;42(10):766-776. doi:10.1002/lsm.20980.

45. Choromańska A, Saczko J, Kulbacka J, Skolucka N, Majkowski M. The potential role of photodynamic therapy in the treatment of malignant melanoma--an in vitro study. *Adv Clin Exp Med*. 2012;21(2):179-185. http://www.ncbi.nlm.nih.gov/pubmed/23214281. Accessed October 28, 2014.

46. Davids LM, Kleemann B, Kacerovská D, Pizinger K, Sh K. Hypericin phototoxicity induces different modes of cell death in melanoma and human skin cells . *J Photochem Photobiol B*. 2008;91(2008 Feb 7):2008. doi:10.1016/j.jphotobiol.2008.01.011.

47. Chen KG, Valencia JC, Gillet J-P, Hearing VJ, Gottesman MM. Involvement of ABC transporters in melanogenesis and the development of multidrug resistance of melanoma. *Pigment Cell Melanoma Res*. 2009;22(6):740-749. doi:10.1111/j.1755-148X.2009.00630.x.

48. Nelson JS, McCullough JL, Berns MW. Photodynamic therapy of human malignant melanoma xenografts in athymic nude mice. *J Natl Cancer Inst*. 1988;80(1):56-60. http://www.ncbi.nlm.nih.gov/pubmed/2963136. Accessed October 21, 2014.

49. Nowis D, Makowski M, Stokłosa T, Legat M, Issat T, Gołąb J. Direct tumor damage mech anisms of photodynamic therapy. *Acta Biochim Pol*. 2005;52(2):339-352.

50. Zitvogel L, Casares N, Péquignot MO, Chaput N, Albert ML, Kroemer G. Immune response against dying tumor cells. *Adv Immunol*. 2004;84:131-179. doi:10.1016/S0065-2776(04)84004-5.

51. Almeida RD, Manadas BJ, Carvalho AP, Duarte CB. Intracellular signaling mechanisms in photodynamic therapy. *Biochim Biophys Acta*. 2004;1704(2):59-86. doi:10.1016/j.bbcan.2004.05.003.

52. Kiesslich T, Plaetzer K, Oberdanner CB, Berlanda J, Obermair FJ, Krammer B. Differential effects of glucose deprivation on the cellular sensitivity towards photodynamic treatment-based production of reactive oxygen species and apoptosis-induction. *FEBS Lett*. 2005;579(1):185-190. doi:10.1016/j.febslet.2004.11.073.

53. Tammela T, Saaristo A, Holopainen T, et al. Photodynamic ablation of lymphatic vessels and intralymphatic cancer cells prevents metastasis. *Sci Transl Med*. 2011;3(69):69ra11. doi:10.1126/scitranslmed.3001699.

54. Huang Y-Y, Vecchio D, Avci P, Yin R, Garcia-Diaz M, Hamblin MR. Melanoma resistance to photodynamic therapy: new insights. *Biol Chem*. 2013;394(2):239-250. doi:10.1515/hsz-2012-0228.

55. Mikeš J, Jendželovský R, Fedoročko P. Cellular Aspects of Photodynamic Therapy with Hypericin. In: Mohamed Lotfy Taha Elsaie, ed. *Photodynamic Therapy: New Research*.; 2013.

56. Theodossiou TA, Hothersall JS, De Witte PA, Pantos A, Agostinis P. The multifaceted photocytotoxic profile of hypericin. *Mol Pharm*. 6(6):1775-1789. doi:10.1021/mp900166q.

57. Van Vliet A, Vepachedu R, Lawrence CB, Stermitz FR, Vivanco JM, Bais HP. Enzyme Catalysis and Regulation : Molecular and Biochemical Characterization of an Enzyme Responsible for the Formation of Hypericin in St . Molecular and Biochemical Characterization of an Enzyme Responsible for the Formation of Hypericin in St . John '. *J Biol Chem*. 2003;278:32413-32422. doi:10.1074/jbc.M301681200.

58. Karioti A, Bilia AR. Hypericins as Potential Leads for New Therapeutics. *Int J Mol Sci*. 2010;11:562-594. doi:10.3390/ijms11020562.

59. Kleemann, B.(2013). *St John's Wort photomedecine for melanoma*. University of Cape Town.

60. Davids LM, Kleemann B. Combating melanoma: the use of photodynamic therapy as a novel, adjuvant therapeutic tool. *Cancer Treat Rev*. 2011;37(6):465-475. doi:10.1016/j.ctrv.2010.11.007.

61. Falk H. From the Photosensitizer Hypericin to the Photoreceptor Stentorin- The Chemistry of Phenanthroperylene Quinones. *Angew Chem Int Ed Engl*. 1999;38(21):3116-3136. http://www.ncbi.nlm.nih.gov/pubmed/10556884. Accessed September 27, 2013.

62. Ott M, Huls M, Cornelius MG, Fricker G. St. John's Wort constituents modulate P-glycoprotein transport activity at the blood-brain barrier. *Pharm Res*. 2010;27(5):811-822. doi:10.1007/s11095-010-0074-1.

63. Butterweck V, Schmidt M. St. John's wort: role of active compounds for its mechanism of action and efficacy. *Wien Med Wochenschr*. 2007;157(13-14):356-361. doi:10.1007/s10354-007-0440-8.

64. Ritz R, Daniels R, Noell S, et al. Hypericin for visualization of high grade gliomas : first clinical experience . *Eur J Surg Oncol*. 2012;38(4):2012. doi:10.1016/j.ejso.2011.12.021.

65. Cole CD, Liu JK, Sheng X, Chin SS, Schmidt MH, Weiss MH CW. Hypericin-mediated photodynamic therapy of pituitary tumors: preclinical study in a GH4C1 rat tumor model. *J Neurooncol*. 2008;87(3):11060. doi:10.1007/s11060-007-9514-0.

66. Hamilton HB, Hinton DR, Law RE, Gopalakrishna R, Su YZ, Chen ZH, Weiss MH CW. Inhibition of cellular growth and induction of apoptosis in pituitary adenoma cell lines by the protein kinase C inhibitor hypericin : potential therapeutic application . *J Neurosurg*. 1996;85(2):329-334.

67. Chung PS, Rhee CK, Kim KH, Paek W, Chung J, Paiva MB, Eshraghi AA, Castro DJ SR. Intratumoral hypericin and KTP laser therapy for transplanted squamous cell carcinoma . *Laryngoscope*. 2000;110(8):1312-1316.

68. Seyed Mohamed Ali MO. Bio-distribution and subcellular localization of Hypericin and its role in PDT induced apoptosis in cancer cells. *Int J Oncol*. 2002;21(3):531-540. doi:10.3892/ijo.21.3.531.

69. Chung PS1, Saxton RE, Paiva MB, Rhee CK, Soudant J, Mathey A, Foote C CD. Hypericin uptake in rabbits and nude mice transplanted with human squamous cell carcinomas : Study of a new sensitizer for laser phototherapy. *Laryngoscope*. 1994;104(12):1471-1476.

70. Huntosova V, Alvarez L, Bryndzova L, et al. Interaction dynamics of hypericin with low-density lipoproteins and U87-MG cells. *Int J Pharm*. 2010;389(1-2):32-40. doi:10.1016/j.ijpharm.2010.01.010.

71. E. M. Delaey, R. Obermuëller, I. Zupkó, D. De Vos HF and PAMDW. In Vitro Study of the Photocytotoxicity of Some Hypericin Analogs on Different Cell Lines. *Photochem Photobiol*. 2007;74(2):164-171. doi:10.1562/0031-8655(2001)0740164IVSOTP2.0.CO2.

72. Kascakova S, Nadova Z, Mateasik A, Mikes J, Huntosova V, Refregiers M. High level of low-density lipoprotein receptors enhance hypericin uptake by U-87 MG cells in the presence of LDL . *Photochem Photobiol*. 2008;84(1):120-127. doi:10.1111/j.1751-1097.2007.00207.x.High.

73. Redmond RW, Gamlin JN. A compilation of singlet oxygen yields from biologically relevant molecules. *Photochem Photobiol*. 1999;70(4):391-475. http://www.ncbi.nlm.nih.gov/pubmed/10546544. Accessed September 27, 2013.

74. Solár P, Cavarga I, Hofmanová J, et al. Effect of acetazolamide on hypericin photocytotoxicity. *Planta Med*. 2002;68(7):658-660. doi:10.1055/s-2002-32902.

75. Kamuhabwa AR, Agostinis PM, D'Hallewin MA, Baert L, de Witte PA. Cellular photodestruction induced by hypericin in AY-27 rat bladder carcinoma cells. *Photochem Photobiol*. 2001;74(2):126-132. http://www.ncbi.nlm.nih.gov/pubmed/11547545. Accessed September 27, 2013.

76. Agostinis P, Buytaert E, Breyssens H, Hendrickx N. Regulatory pathways in photodynamic therapy induced apoptosis. *Photochem Photobiol Sci*. 2004;3(8):721-729. doi:10.1039/b315237e.

77. Oleinick NL, Morris RL, Belichenko I. The role of apoptosis in response to photodynamic therapy: what, where, why, and how. *Photochem Photobiol Sci*. 2002;1(1):1-21. http://www.ncbi.nlm.nih.gov/pubmed/12659143. Accessed September 27, 2013.

78. Davids LM, Kleemann B, Kacerovská D, Pizinger K, Kidson SH. Hypericin phototoxicity induces different modes of cell death in melanoma and human skin cells. *J Photochem Photobiol B*. 2008;91(2-3):67-76. doi:10.1016/j.jphotobiol.2008.01.011.

79. Kessel D, Luo Y, Deng Y, Chang CK. The role of subcellular localization in initiation of apoptosis by photodynamic therapy. *Photochem Photobiol*. 1997;65(3):422-426. http://www.ncbi.nlm.nih.gov/pubmed/9077123.

80. Gupta V, Su YS, Wang W, et al. Enhancement of glioblastoma cell killing by combination treatment with temozolomide and tamoxifen or hypericin. *Neurosurg Focus*. 2006;20(4):E20. doi:10.3171/foc.2006.20.4.13.

81. Bradbury PA, Middleton MR. DNA repair pathways in drug resistance in melanoma. *Anticancer Drugs*. 2004;15(5):421-426. http://www.ncbi.nlm.nih.gov/pubmed/15166615. Accessed September 27, 2013.

82. Koprowska K, Hartman ML, Sztiller-Sikorska M, Czyz ME. Parthenolide enhances dacarbazine activity against melanoma cells. *Cancer Biol Ther*. 2013;24(8):835-845. doi:10.1097/CAD.0b013e3283635a04.

83. Boeckmann L, Schirmer M, Rosenberger A, et al. Effect of DNA repair host factors on temozolomide or dacarbazine melanoma treatment in Caucasians. *Pharmacogenet Genomics*. 2009;19:760-769. doi:10.1097/FPC.0b013e3283307cd9.

84. Mf S, Ja H, Sp L, et al. Antitumor activity and pharmacokinetics in mice of 8-carbamoyl-3-methyl-imidazo[5,1-d]-1,2,3,5-tetrazin-4(3H)-one (CCRG 81045; M & B 39831), a novel drug with potential as an alternative to dacarbazine. *Cancer Res*. 1987;47(22):5846-5852.

85. Serrone L, Zeuli M, Fm S, Cognetti F. Dacarbazine-based chemotherapy for metastatic melanoma : thirty-year experience overview . *J Exp Clin Cancer Res*. 2000;19(1):21-34.

86. Kaina B, Christmann M, Naumann S RW. MGMT: key node in the battle against genotoxicity, carcinogenicity and apoptosis induced by alkylating agents. *DNA Repair*. 2007;6(8):1079-1099.

87. Roos W, Baumgartner M, Kaina B. Apoptosis triggered by DNA damage O6-methylguanine in human lymphocytes requires DNA replication and is mediated by p53 and Fas / CD95 / Apo-1 . *Oncogene*. 2004;23(2):359-367.

88. Palathinkal DM, Sharma TR, Koon HB, Bordeaux JS. Current systemic therapies for melanoma. *Dermatol Surg*. 2014;40(9):948-963. doi:10.1097/01.DSS.0000452626.09513.55.

89. Ugurel S, Paschen A, Becker JC. Dacarbazine in melanoma: from a chemotherapeutic drug to an immunomodulating agent. *J Invest Dermatol*. 2013;133(2):289-292. doi:10.1038/jid.2012.341.

90. Luo Y, Ellis LZ, Dallaglio K, et al. Side Population Cells from Human Melanoma Tumors Reveal Diverse Mechanisms for Chemoresistance. *J Invest Dermatol*. 2012;132(10):2440-2450. doi:10.1038/jid.2012.161.

91. Valero T, Steele S, Neumüller K, et al. Combination of dacarbazine and dimethylfumarate efficiently reduces melanoma lymph node metastasis . *J inverstigative dermatologytigative dermatology*. 2010;130(4):1087-1094. doi:10.1038/jid.2009.368.

92. THRALL BD, RAHA GA, SPRINGER DL, GARY G. MEADOWS. Differential Sensitivities of Murine Melanocytes and Melanoma Cells to Buthionine Sulfoximine and Anticancer Drugs. *Pigment Cell Res*. 1991;5-6(4):234-239.

93. Wouters J, Stas M, Gremeaux L, et al. The human melanoma side population displays molecular and functional characteristics of enriched chemoresistance and tumorigenesis. *PLoS One*. 2013;8(10):e76550. doi:10.1371/journal.pone.0076550.

94. Luo Y, Ellis LZ, Dallaglio K, et al. Side population cells from human melanoma tumors reveal diverse mechanisms for chemoresistance. *J Invest Dermatol*. 2012;132(10):2440-2450. doi:10.1038/jid.2012.161.

95. Chen KG, Valencia JC, Lai B, et al. Melanosomal sequestration of cytotoxic drugs contributes to the intractability of malignant melanomas. *Proc Natl Acad Sci U S A*. 2006;103(26):9903-9907. doi:10.1073/pnas.0600213103.

96. Jones PM, George a M. The ABC transporter structure and mechanism: perspectives on recent research. *Cell Mol Life Sci*. 2004;61(6):682-699. doi:10.1007/s00018-003-3336-9.

97. Dean M, Hamon Y, Chimini G. The human ATP-binding cassette (ABC) transporter superfamily. *J Lipid Res*. 2001;42(7):1007-1017. http://www.ncbi.nlm.nih.gov/pubmed/11441126.

98. Dean M. ABC Transporters , Drug Resistance , and Cancer Stem Cells. *J mammary Gland Biol Neoplasia*. 2009;14:3-9. doi:10.1007/s10911-009-9109-9.

99. Morita M, Imanaka T. Peroxisomal ABC transporters: structure, function and role in disease. *Biochim Biophys Acta*. 2012;1822(9):1387-1396. doi:10.1016/j.bbadis.2012.02.009.

100. Molinari A, Alcabrini AC, Eschini SM, et al. DETECTION OF P-GLYCOPROTEIN IN THE GOLGI APPARATUS OF DRUG-UNTREATED HUMAN MELANOMA CELLS. *Int J cancer*. 1998;75(November 1997):885-893.

101. Frank NY, Margaryan A, Huang Y, et al. ABCB5-Mediated Doxorubicin Transport and Chemoresistance in Human Malignant Melanoma. *Cancer Res*. 2005;65(10):4320-4333.

102. Wu C-P, Sim H-M, Huang Y-H, et al. Overexpression of ATP-binding cassette transporter ABCG2 as a potential mechanism of acquired resistance to vemurafenib in BRAF(V600E) mutant cancer cells. *Biochem Pharmacol*. 2013;85(3):325-334. doi:10.1016/j.bcp.2012.11.003.

103. Bebes A, Nagy T, Bata-Csörgo Z, Kemény L, Dobozy A, Széll M. Specific inhibition of the ABCG2 transporter could improve the efficacy of photodynamic therapy. *J Photochem Photobiol B*. 2011;105(2):162-166. doi:10.1016/j.jphotobiol.2011.08.007.

104. Robey RW, Steadman K, Polgar O, Bates SE. ABCG2-mediated transport of photosensitizers: potential impact on photodynamic therapy. *Cancer Biol Ther*. 2005;4(2):187-194.

105. Liu W, Baer MR, Bowman MJ, et al. The Tyrosine Kinase Inhibitor Imatinib Mesylate Enhances the Efficacy of Photodynamic Therapy by Inhibiting ABCG2 The Tyrosine Kinase Inhibitor Imatinib Mesylate Enhances the Efficacy of Photodynamic Therapy by Inhibiting ABCG2. *Clin Cancer Res*. 2007;13(8):2463-2470. doi:10.1158/1078-0432.CCR-06-1599.

106. Goler-Baron V, Assaraf YG. Overcoming multidrug resistance via photodestruction of ABCG2-rich extracellular vesicles sequestering photosensitive chemotherapeutics. *PLoS One*. 2012;7(4):e35487. doi:10.1371/journal.pone.0035487.

107. Gottesman MM, Fojo T, Bates SE. Multidrug resistance in cancer: role of ATP-dependent transporters. *Nat Rev Cancer*. 2002;2(1):48-58. doi:10.1038/nrc706.

108. Abel E V, Aplin AE. Finding the root of the problem: the quest to identify melanoma stem cells. *Front Biosci (Schol Ed)*. 2011;3:937-945. http://www.ncbi.nlm.nih.gov/pubmed/21622243. Accessed September 27, 2013.

109. Setia N, Abbas O, Sousa Y, Garb JL, Mahalingam M. Profiling of ABC transporters ABCB5 , ABCF2 and nestin-positive stem cells in nevi , in situ and invasive melanoma. *Mod Pathol*. 2012;25(8):1169-1175. doi:10.1038/modpathol.2012.71.

110. Touil Y, Zuliani T, Wolowczuk I, et al. The PI3K/AKT signaling pathway controls the quiescence of the low-Rhodamine123-retention cell compartment enriched for melanoma stem cell activity. *Stem Cells*. 2013;31(4):641-651. doi:10.1002/stem.1333.

111. Czyz M, Koprowska K, Sztiller-sikorska M. Parthenolide reduces the frequency of ABCB5-positive cells and clonogenic capacity of melanoma cells from anchorage independent melanospheres. *Cancer Biol Ther*. 2013;14(2):135-145.

112. Tolleson WH. Human melanocyte biology, toxicology, and pathology. *J Environ Sci Health C Environ Carcinog Ecotoxicol Rev*. 2005;23(2):105-161. doi:10.1080/10590500500234970.

113. Jendˇ R, Souˇ K, Saˇ V, Kozub A, Fedoroˇ P. Drug efflux transporters , MRP1 and BCRP , affect the outcome of hypericin-mediated photodynamic therapy in HT-29 adenocarcinoma cells. 2009:1716-1723. doi:10.1039/b9pp00086k.

114. Robey RW, Steadman K. ABCG2-Mediated Transport of Photosensitizers. *Cancer Biol Ther*. 2005;4(2):187-194.

115. Ishikawa T, Nakagawa H, Hagiya Y, Nonoguchi N, Miyatake S, Kuroiwa T. Key Role of Human ABC Transporter ABCG2 in Photodynamic Therapy and Photodynamic Diagnosis. *Adv Pharmacol Sci*. 2010;2010:1-13. doi:10.1155/2010/587306.

116. Hirose K, Longo DL, Oppenheim JJ, Matsushima K. Overexpression of mitochondrial manganese superoxide dismutase promotes the survival of tumor cells exposed to interleukin-1, tumor necrosis factor, selected anticancer drugs, and ionizing radiation. *FASEB J*. 1993;7(2):361-368. http://www.ncbi.nlm.nih.gov/pubmed/8440412.

117. Sparsa A, Bellaton S, Naves T, et al. Photodynamic treatment induces cell death by apoptosis or autophagy depending on the melanin content in two B16 melanoma cell lines. *Oncol Rep*. 2013;29(3):1196-1200. doi:10.3892/or.2012.2190.

118. Adar Y, Stark M, Bram EE, et al. Imidazoacridinone-dependent lysosomal photodestruction : a pharmacological Trojan horse approach to eradicate multidrug-resistant cancers. *Cell Death Dis*.2012;3(4):e293-10. doi:10.1038/cddis.2012.30.

119. Frank NY, Margaryan A, Huang Y, et al. ABCB5-Mediated Doxorubicin Transport and Chemoresistance in Human Malignant Melanoma in Human Malignant Melanoma. *Cancer Res*. 2005:4320-4333.

120. Keshet GI, Goldstein I, Itzhaki O, et al. MDR1 expression identifies human melanoma stem cells. *Biochem Biophys Res Commun*. 2008;368(4):930-936. doi:10.1016/j.bbrc.2008.02.022.

121. Monzani E, Facchetti F, Galmozzi E, et al. Melanoma contains CD133 and ABCG2 positive cells with enhanced tumourigenic potential. *Eur J Cancer*. 2007;43(5):935-946. doi:10.1016/j.ejca.2007.01.017.

122. Meszaros P, Hummel I, Klappe K, Draghiciu O, Hoekstra D, Kok JW. The function of the ATP-binding cassette (ABC) transporter ABCB1 is not susceptible to actin disruption. *Biochim Biophys Acta*. 2013;1828(2):340-351. doi:10.1016/j.bbamem.2012.10.007.

123. Fukunaga-Kalabis M, Herlyn M. Beyond ABC: another mechanism of drug resistance in melanoma side population. *J Invest Dermatol*. 2012;132(10):2317-2319. doi:10.1038/jid.2012.220.

124. Brenner MK. A distinct "' side population '" of cells with high drug efflux capacity in human tumor cells. *Proc Natl Acad Sci U S A*. 2004;101(39):14228-14233.

Appendices

A. Dulbecco's modified Eagle's medium (DMEM)

Weight out DMEM powder: 27,1g and $NaHC0_2$: 7.4g

Measure out 90% 1800ml of dH_20

Add powders and stir

Make up water up to 2L

Adjust pH to 7.4

Filter sterilise immediately using a 0.22µ filter

Aliquot into 500ml bottles

Store at 4°C

B. Heat inactivation of Fetal Calf serum (FCS)

Thaw FCS

Heat at 56°C for 20min

Cool to room temperature

Store at -20°C

C. Antibiotics: Penicillin/Streptomycin

Weight out: 6mg penicillin and 10mg od streptomycin

Dissolve in 1L of dH_20

Sterile filter through 0.22µ filter

Aliquot out working volumes

Store at -20^{o}C

Dilute 1:100 for routine use.

D. Hypericin

Hypericin stock (2mM) is made up in DMSO and stored at -80^{o}C

Working stock 20µM is made up in 1xPBS

Equation used to calculate relative volumes of hypericin

Ci x Vi= Cf x Vf for 3µM of HYP

E. Dacarbazine (DTIC)

DTIC working stock (10mM) is made up in 0.9% NaCl and stored at -20^{o}C

It is made by weighing out 0.018218g of DTIC and dissolving it into 10ml

0.9% NaCl

Equation used to calculate relative volumes of DTIC

Cix Vi = Cf x Vf for the various DTIC concentrations

F. Phosphate Buffer Saline (1xPBS, pH 7.4)

Weigh out: 8g NaCl (0.14M); 1.26g Na_2HPO_4 anhydrous (8.8M); 0.2g KCL (2.7M); 0.2g KH_2PO_4 (1.47M)

Dissolve the above in 800ml dH_20

Adjust pH to 7.4

Add dH_20 up to 1L

Autoclave in 500ml bottles

G. Trypsin (0.05%)/ EDTA (0.02%) in 1xPBS

Weigh out 0.05g Trypsin and 0.02g EDTA

Dissolve trypsin in 100ml PBS

Add EDTA and dissolve

Sterilise by filtering through 0.22µ filter

Aliquot into 50ml tubes

Store at -20^oC

H. Components of RIPA complete extraction buffer

CPIC tablets (complete Protease inhibitor Tablets)

Dissolve 1 tablet in 2ml dH_20 for a 25x stock

Aliquot (100µl) and store at -20^oC

Pepstatin (comes as liquid)

Aliquot (100µl) and stored at -20^oC

Aproptonin

Powder stored at 4°C

Dissolve 1mg powder in 1m dH_20

Aliquot (100µl) and store at -20°C

0.1M PMSF (phenylmethylsulfonicfluoride)

Dissolve 0.087g in 5ml isopropanol

Store in a dark bottle at RT or aliquot (100µl) and store at -20°C

I. RIPA buffer (in 50ml)

From each stock:

Take 1.5ml of NaCl (5M)

Add 500µl of Triton X-100 (100%)

500µl SDS (10%)

1ml Tris, pH 7.5 (1M)

Add 0.5g Deoxycholate

Add 46.5ml dH_20

Filter sterilise through a 0.45 filter

Store in aliquots at 4°C

J. RIPA Complete Extraction Buffer (500µl)

From each stock:

Take 20µl CPIC (25x)

Add 0.5µl Aproptinin (1mg/ml)

2.5µl PMSF (100mM)

0.5µl Pepstatin A

And 476µl RIPA buffer

K. Western blotting

Resolving gel buffer (1.5M Tris pH 8.8, 0.4% SDS)

Weigh out: 36.342g Tris and 0.8g SDS

(Wear mask when weighing out!! Be careful)

Add it in 190ml dH_20

Heat slightly to dissolve (+/- 190ml)

Add 180 drops concentrated HCL to pH

Then make up to 200ml final volume

Store at 4^oC

Stacking gel buffer (0.5M Tris pH 6.8, 0.4% SDS)

Weigh out: 6.057g tris

Add 0.4g SDS (wear mask when weighing out)

Add 90ml of ddH_20

10x Running buffer (0.25M Tris, 1.92M Glycine, 1% SDS)

Weigh out: 30.2g Tris and 144g Glycine

10g SDS (wear mask when weighing out)

Make up to 1L with ddH_20

1x Running buffer (0.025M Tris, 0.192M Glycine, 0.01%SDS)

Take 100ml of 10x running buffer

Add 900ml of ddH_20

10x Transfer buffer (0.31M Tris, 1.92M Glycine)

Weigh out: 144g glycine and 38g of Tris

Make up to 1L with ddH_20

Store at 4^oC

1x Transfer buffer (0.031M Tris, 0.192M Glycine)

Take 100ml of 10x Transfer buffer

Add to it 700ml ddH_20

Then, add methanol/isopropanol (methanol can be technical grade)

10x Tris Buffered Saline (TBS) pH 7.5

Weigh out: 60.5g Tris and 87.6g NaCl

Dissolve in 700ml of ddH_20

Then pH to 7.5

Make up to 1L

1x TBS-Tween

Take 100ml of 10x TBS pH 7.5

Add 900ml of ddH_20

Add 1ml Tween20

5x Loading Buffer (LB)

Weigh out 1.75g Tris

Add 30ml of glycerine

Make it up to 40ml with ddH_20

pH it to 6.8 with 1N HCL

Add 5g SDS/SLS

Make up to 50ml

5x Loading dye

Heat up 5x loading buffer to allow SDS precipitate to dissolve

Mix with 100µl 5x loading buffer (2 parts)

50µl β-mercaptoethanol (1 part)

50µl 0.025% bromophenol blue (1 part)

Use at 1x loading dye on the gel.

Ponceau S stain (0.1% (w/v) ponceau S in 5% (v/v) acetic acid)

Weigh 1g Ponceau S

Add 50ml acetic acid

Make up to 1L with ddH_20

Store at 4^oC. Do not freeze